2010

A Theoretical Model of the Effect of Bone Defects on Anterior Shoulder Instability: a Finite Element Approach

Piyush Walia
Cleveland State University

A THEORETICAL MODEL OF THE EFFECT OF BONE DEFECTS ON ANTERIOR SHOULDER INSTABILITY: A FINITE ELEMENT APPROACH

PIYUSH WALIA

Bachelors of Technology in Mechanical Engineering

Chandigarh Engineering College

May, 2007

Submitted in partial fulfillment of requirements for the degree
MASTER OF SCIENCE IN BIOMEDICAL ENGINEERING
at the
CLEVELAND STATE UNIVERSITY
December, 2010

This thesis has been approved

For the Department of Chemical and Biomedical Engineering

and the college of Graduate Studies by

_____

Thesis Chairperson, Stephen D. Fening

_____

Department & Date

_____

Dr. Majid Rashidi

_____

Department & Date

_____

Dr. Ahmet Erdemir

_____

Department & Date

ACKNOWLEDGMENTS

I would like to thank my advisor and mentor Dr. Stephen D. Fening for his support and guidance during my research for my thesis. He had been very kind and patient while suggesting me the outlines of this project and correcting my mistakes. I would also like to thank my committee members, Dr. Majid Rashidi, Dr. Ahmet Erdemir and Dr. Anthony Miniaci for their insight and knowledgeable support. I would also like to acknowledge my colleague Scott Sibole for helping me with various questions I had throughout my research.

Finally, I would like to thank my best friend for helping me and standing by me in the hard times and my parents for motivating me.

A THEORETICAL MODEL OF THE EFFECT OF BONE DEFECTS ON ANTERIOR SHOULDER INSTABILITY: A FINITE ELEMENT APPROACH

PIYUSH WALIA

ABSTRACT

Presence of either a Hill Sachs or a Bony Bankart lesion has been indicated as a possible cause of subluxation and anterior shoulder dislocation. Previous studies have investigated only effects of these isolated lesions on the glenohumeral instability of the shoulder. The purpose of this thesis was to investigate the effect of both Bony Bankart lesion and Hill-Sachs lesion in the glenohumeral joint on the stability of the shoulder. We hypothesize that as the size of the lesion increases, the glenohumeral joint's stability will decrease. We further hypothesize that the presence of both defects together will reduce the glenohumeral joint's stability to an even greater extent. Finite element analysis approach was utilized to model the glenohumeral joint in combination with the intact humerus and the glenoid. The model was developed for the cartilage and the bone of the glenoid and the humerus, using the data from classical research papers. Different sets of simulation were run with both isolated and combined defects to analyze the reaction forces and calculate distance to dislocation. The experiments were analyzed using statistical analysis with displacement control. The results from the study predicted a theoretical model which explains the direct correlation between the anterior stability of glenohumeral joint and the size of the defect. It was found that, with the increase in size of the defect, the distance to dislocation decreased and so does the stability. Presence of both the lesions simultaneously further decreased the glenohumeral stability, for some cases it decreased to zero percent. This data was consistent with our second hypothesis.

TABLE OF CONTENTS

LIST OF TABLES

Page No.

LIST OF FIGURES

Page No.

NOMENCLATURE

R	Radius of the circle	m
R_g	Radius of the glenoid	m
R_h	Radius of humeral head	m
E	Young's Modulus of Elasticity	Pa or N/m^2
ν	Poisson's ratio	
C_{10}	The neo-Hookean material constant	Pa or N/m^2
D_{10}	The neo-Hookean material constant	Pa or N/m^2
Fx	Reaction force in x-direction of the global coordinates	N
RFH	Peak reaction force acting on the humerus in x-direction	N

CHAPTER I

INTRODUCTION

The shoulder's glenohumeral joint is vital to performing activities of daily living, which often require a great range of motion. This joint sustains large amounts of strain during repeated motion in aggressive activities, such as professional sports. Being the most mobile joint in the body, it allows one to move his or her shoulder through a wide arc of motion. One can adduct and abduct his or her shoulder at different angles, providing external and internal rotation of the arm. The glenohumeral joint permits a wider range of motion than any other joint in the body, and provides stability and flexibility in activities like baseball pitching, wrestling, and tennis (Figure -1).

Figure 1. Some activities showing different range of motion of shoulder.

The primary drawback to the large range of motion of the glenohumeral joint is tendency to become pathologically unstable. Instability can result a fall or impact while participating in sports. In the United States, approximately 1.7% of the general population experiences anterior shoulder dislocation.[65] Similar injuries are seen more frequently during contact sports and military activities. The incidence of dislocation in athletes has been reported to be near 4-5% by Owens et al.[48] Such a high rate of dislocations among general population and athletes is a matter of concern for sports medicine. Insufficient knowledge about treatment options is due to a lack of research on joint stability and repair procedures to restore stability. Thus, there is a need for further research studies addressing shoulder instability.[42, 62] Recurrent dislocation is commonly seen in baseball pitchers, football players and downhill skiers, because these sports indulge a lot of pressure on the shoulder shown in Figure 2 below.

Figure 2. Some activities involving extreme load conditions on the shoulder.

Instability of the shoulder is described as the condition which can lead to recurrent dislocation of the shoulder. It is believed that the glenohumeral joint's instability is primarily a result of two factors. First, is the natural anatomy of the glenohumeral joint, which has a great mismatch between the articular surface of humeral head and glenoid; the humerus being larger.[59] The glenoid fossa's shallowness also contributes to instability and the glenoid's smaller surface area of contact leads to abnormalities.[24, 37, 41, 59] The second factor is injury due to trauma. The reasons for trauma can be a direct fall on the shoulder or a sports related injury. The other reasons described by Bigliani et al. for the occurrence of the shoulder's instability are the laxity of the rotator cuff muscle, defects in the connective tissues and repeated injury leading to the chronic disorders.[8] Repeated dislocation due to unsuccessful surgery can also lead to osteoarthritis.

During an acute injury a compression fracture can occur in the bony surface of the glenoid or humeral head. The two common bony lesions leading to glenohumeral instability are the Hill Sachs lesion and Bony Bankart lesion.[17] The Hill Sachs defect is a grooved defect with loss of bone from the upper tuberosity of the humeral head,

described by Hill and Sach in 1940.[22] A Bony Bankart lesion is the detachment of the glenoid labrum from the glenoid rim and loss of bone at the glenoid rim.[52] Treatment for both of these types of lesions may require repair of the bone defect or even total shoulder replacement, depending upon the size and nature of the defect.[8, 27, 28, 39, 40] The most common method for the treatment is isolated soft tissue repair, where bone defects are left untreated. This is due to the fact that little evidence based guidelines for the treatment of bony defects. Surgeries are tedious and time consuming. Therefore, further data is needed to convince the surgeon to perform surgery instead of tissue repair.

The study by Rowe et al. found that there has been nearly 76% of cases of shoulder dislocation with Hill Sachs defect, 84% with the Bony Bankart lesion and 31% had both Bony Bankart and Hill Sachs defect.[53] Another study by Flinkkia et al. found that the incidence of recurrent instability for 182 patients from their study was approximately 19%.[19] Recent research has focused on predicting the effect of the Bony Bankart lesion and the Hill-Sachs defect on glenohumeral joint's instability. Some studies by authors like Itoi et al., Iannotti et al., Sekiya et al. and Kaar et al. have shown the adverse effects of lesions on the stability of glenohumeral joint.[9, 27, 32, 56] Also an inverse relationship has been found between the distance to dislocation and size of the defect. There have been many controversies regarding treatment options for the shoulder defects, due to limited data. While these studies have begun to answer fundamental questions for situations where an isolated defect is present, it is most common to have a defect on both the humeral head and glenoid.[64] No study has evaluated the effects of the glenohumeral joint's stability due to the presence of both Hill Sachs and Bony Bankart lesion simultaneously. Many authors have commented that glenohumeral stability will decrease

if both the lesions are present together. Studying the effects of combined defects in glenohumeral joint will help us better understand the shoulder's stability. Further research will help gain information about better surgical techniques and treatment options for different lesions present in the joint.

The complex anatomy of the glenohumeral joint limits the ability of researchers to investigate mechanically both Hill Sachs and Bony Bankart lesions together in a cadaver study. The high cost related to more number of specimens and complex equipment required for the cadaveric study is another disadvantage. The aim of this study was to show a theoretical relationship between combined defects and shoulder stability. To achieve our objective, a finite element representation of the glenohumeral joint was developed and static translational analyses were performed. Various combination of the defects sizes at two different abduction angles of arms were simulated to observe changes in stability. The novelty of this study is that it addresses the specific case when the combined effects of Bony Bankart and Hill Sachs lesions are encountered, through a finite element analysis approach. The results from this study will be beneficial for the surgical treatment of shoulder stability. This will enable the patient to return back to a normal state of stability and ultimately, reduce the need for repeated shoulder surgeries. We hypothesize that as the size of the lesion increases, the glenohumeral joint's stability will decrease. We further hypothesize that presence of both defects together will reduce the glenohumeral joint's stability to an even greater extent than the presence of an individual defect.

Background

1.1 Anatomy of the shoulder

The shoulder is made up of different bones, joints, ligaments and capsule. The different joints of a shoulder complex are Scapulothoractic joint, Sternoclavicular joint, Acromioclavicular joint and Glenohumeral Joint. The other components are Scapular Ligaments, and Glenohumeral capsule. The bony anatomy of the shoulder includes Humerus, Scapula and Clavicle as shown in Figure 3.[59] The different components are described below.

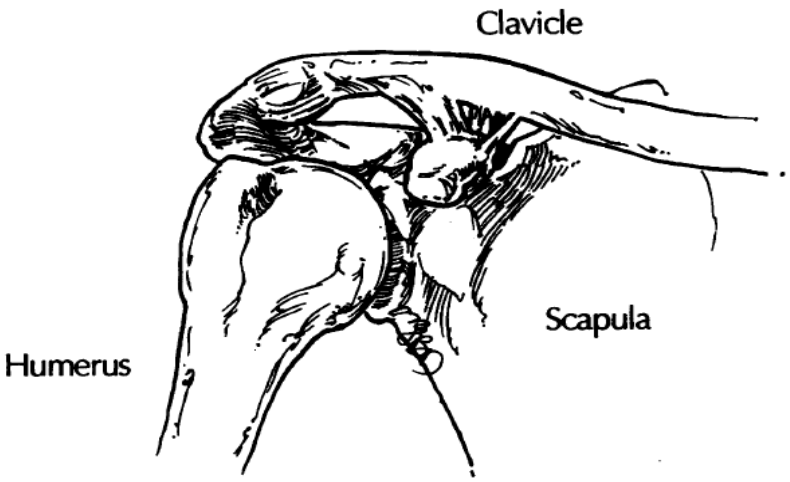

Figure 3. Various components of shoulder are humerus, clavicle, and scapula.[59]

1.1.1 Humerus

The humerus is the longest bone in the upper extremity of a body, whose head is similar to shape of a half spheroid. The head of the humerus is inclined with the shaft of the bone at an angle of about 130º at the anatomical neck and has a retroversion angle of 26º to 31º from the medial and lateral epicondylar plane[34, 49, 59]. The humerus is

considered to have more surface area of contact as compared to glenoid[41]. In the contact sports, sometimes the substantial force acting on the shoulder can lead to the glenohumeral joint's dislocation. It can happen with or without the possibility of fracture at proximal humeral head. The defect in the upper tuberosity of the humerus is called the Hill Sachs lesion. The problem of the humerus fracture increase with age after 40 years due to the osteoporosis[59].

1.1.2 Scapula

Scapula is a "thin and large triangle shape bone situated on the posterolateral aspect of the thorax", overlying ribs which serves as a point of attachment for different muscles.[59] It has some soft tissues which provide little cushioning that may lead to the fractures through indirect trauma. The base of the acromion is formed by the superior and lateral extension of the supraspinatus muscle which is separated from infraspinatus by the superior process or spine.[16] The spine has the function of the insertion of the trapezium muscle and as the origin point of the posterior deltoid muscle.[59] The acromion serves as the function of the lever arm of the deltoid which articulates with the distal end of the clavicle. The acromion form the roof surface for the rotator cuff, any variations in the acromial surface can cause wear of the rotator cuff causing impingements.[59] These types of impingements are most commonly seen in the overhead athletes due to repeated movements.[62] The role of the scapula is to act as a linkage between the proximal and distal parts of the body. It also provides the motion along the thoracic wall.[16]

1.1.3 Clavicle

The clavicle is a bony strut which provide connection between "the trunk and the shoulder girdle via the sternoclavicular joint medially and acromioclavicular joint

laterally".[59] The long axis of the clavicle has been found to have double curves. The tubular medial third is able to take some axial loading and the flat outer third portion is helpful in the attachment of the muscles and the ligaments. The middle third area is considered to be weak being very thin, which can be the reason why it's more prone to fractures. The clavicle has many advantages, it helps to protect neurovascular structure by acting as a barrier, it also helps to stabilize the shoulder complex from displacing from its original position and it act as a point for the attachment of various muscles and ligaments.[59] An injury between the scapula and clavicle of the joint can lead to shoulder separation. The Figure 4 below shows components of the shoulder joint.

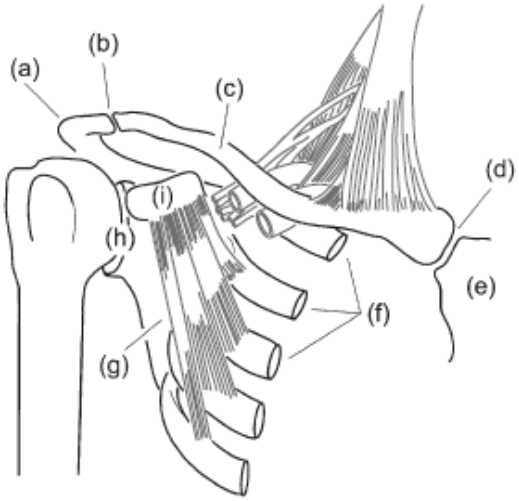

Figure 4. The different joints of the shoulder are (a) Acromion process; (b) Acromioclavicular joint; (c) Clavicle; (d) Sternoclavicular joint; (e) Sternal manubrium; (f) 1st through 3rd Ribs; (g) Scapulothoracic joint; (h) Glenohumeral joint; (i) Coracoid process.[57]

1.1.4 Glenohumeral joint

The glenohumeral joint comprises the concave glenoid fossa of the scapula and the sphere shaped humeral head.[57] This joint is similar to a ball- socket joint. The stability of the shoulder is provided by many static and dynamic stabilizers.[2, 46, 59] Other static stabilizers working in conjunction with the glenohumeral joint are as follows: glenohumeral ligaments and the glenoid labrum which is the fibro-cartilaginous rim attached around the margin of the glenoid cavity.[3, 13, 46, 57] The dynamic stabilizers are the muscles and tendons of the rotator cuff.[2] These all contribute to stabilization of the shoulder in static and dynamic loading. The glenohumeral joint is largely mobile despite its mismatch between the articular surface of the humeral head and glenoid; the humerus being larger. The humeral head has approximately 20-30% of contact with the glenoid fossa at any given time.[54, 59] In the glenohumeral joint, the humeral head is precisely constrained within 1-2 mm of the center of the glenoid during the rotation and arc of motion.[2, 59] The muscle forces acting on the humerus produces concavity compression effects directed towards the glenoid center. The stabilizing effect is produced by the articular surface and capsulolabral.[38, 59] Concavity compression is described to be an important stabilization principle for the glenohumeral joint. Lippitt et al also made some efforts to explain the other stabilizing principle of the joint and they called it: scapulohumeral balance.[38] They described this principal as balancing act involving a large round ball and seal, stating that the "seal position a ball on its nose so that the weight of the ball stay in line with nose".[38] Similarly the humeral head is balanced in the glenoid if the net joint reaction forces passes through the glenoid fossa. Whenever there is abnormality or change in the bony anatomy of the glenohumeral joint due to injury or

trauma, the shoulder's instability can be seen. Muscles associated with the glenohumeral joint are the deltoid muscle and the rotator cuff muscle, which are discussed below.

The deltoid muscle is an important component of the shoulder. Being the largest muscle in this region, it converges to humerus shaft and covers a majority of the proximal portion of the humerus.[16] Deltoid muscle provides largest movement to the arm during elevation.[35] It also has a large correctional area as well.[6, 16] Rotator cuff (also a muscle) helps the arm to move in the space, these are located below the deltoid muscle. Rotator cuff comprises of four muscles, which are the subscapularis, the supraspinatus, the infraspinatus, and the teres minor.[16] The most powerful rotator cuff muscle is the subscapularis muscle. The rotator cuff provides stability to the shoulder through the mechanisms of joint compression and coordinated contraction of the rotator cuff. The humeral head is guided into the glenoid through full range of motion.[37] Another part of the glenohumeral joint is the glenoid labrum; it is the fibrocartilage ring that is present on the circumference of the glenoid fossa.[57] The labrum cartilage is comprised of collagen fibers layers, which provides cushioning and stabilization effect.[57] It tends to increase the extent of the conforming articular surface, which further increases the area of contact, providing stability to the joint.[59] Cartilage allows the smooth frictionless rotation between the glenoid and humeral head. One of the important roles of the labrum is that it increases the depth of the glenoid in the anteroposterior from 2.5 to 5 mm and in the superior-inferior plane concavity is deepened by 9 mm. The glenohumeral ligamentous is attached to fibrocartilagious ring.[24, 37]

1.1.5 Glenohumeral capsule

The glenohumeral capsule permits the unrestricted movement of the glenohumeral joint, which is strengthened by the rotator cuff and other glenohumeral ligaments.[3, 13, 57] The capsule is a specialized space which includes the superior glenohumeral ligament, the middle glenohumeral ligament, the anterior band of the inferior glenohumeral ligament and the posterior band of the inferior glenohumeral joint.[3, 43] The capsule has larger surface area, about twice the surface area of the humeral head. 'The anterior of the capsule has distinct thickenings called glenohumeral ligaments'.[41] The ligaments act as the static stabilizer for the glenohumeral joint.[46, 57] The study by O'Brien et al. also stated that earlier the ligaments were considered as thickening in the glenohumeral joint capsule but now they are proven to play an important role in the glenohumeral joint's stability.[46] Recently, the coracohumeral ligament has been discovered to have a greater surface area than the superior glenohumeral ligament, and coracohumeral ligament has more strength and loading capacity.[37] In conclusion, they all are equally important in glenohumeral joint.

The superior glenohumeral and the coracohumeral ligament functions simultaneously to limit the inferior translation and the external rotation in an adducted arm. The coracohumeral ligament is parallel to the superior glenohumeral ligament which helps in restricting the translation movement. When the arm is adducted, the middle glenohumeral ligament limits the external rotation and inferior translation and also limits the anterior translation with arm abducted at 45º having external rotation.[46] Another ligament, the inferior glenohumeral ligament has been found to comprise of two parts, i.e. a superior band and an axillary pouch.[46, 60] The inferior glenohumeral ligament has the

function of static stabilizer when the arm is rotated externally and abducted to 45º to 90º. Some other important functions of the capsule are support for the synovial membrane, act as a restraint, a watertight seal, and provide an extension of periarticular tendon insertions.[13] The Figure 5 shows the various components and ligaments of the shoulder joint complex.

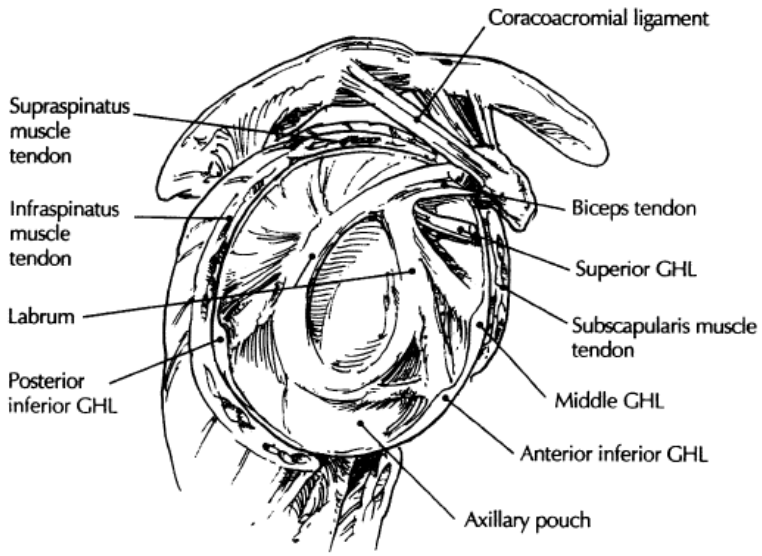

Figure 5- Glenohumeral joint ligaments.[41]

1.2 Normative glenohumeral joint anatomy

For modeling the glenohumeral joint for experimental analysis we require the radius of the curvature of the articular bones and the articular cartilage. These dimensions were taken from the literature data available from classical research papers. We assumed the approximate geometry of the glenoid and humerus and based our study on the sample data available from the past studies. The size of the glenoid was also taken from previous research done by peer researchers. The work done by researchers like Louis J Soslowsky et al., JP Iannotti et al., L. F. De Wilde et al., Mallon et al., Jobe et al., Wataru et al., and

Kelkar et al contributed to gather important information about the shape, geometry, and size of various components of the glenohumeral joint.[12, 14, 26, 31, 33, 39, 44, 58, 61, 63] For our study, we chose the radius of curvature of the glenoid bone to be 34.56 mm and the radius of the curvature of the glenoid cartilage to be 26.37 mm taken from the study done by Soslowsky et al. These values were taken from the data of the male population with ages ranging from 49 to 90 years, average age being 72 years.[26, 49, 58] The radius of curvature for the humerus articular bone is 26.10 mm and the radius of curvature of the cartilage for the humeral head is 26.85 mm.[26, 58] The other dimensions of the glenoid have been adequately described by authors like Iannotti et al., Wilde et al., Kwon et al., and others.[14, 26, 36] From the previous research, the dimension of the superior-inferior is 39 ± 3.5 mm and the dimension of the anterior-posterior position is 29 ± 3.2mm, i.e. distance between A-B and C-D as shown in the Figure 6.[7, 14, 26, 30, 36, 39]

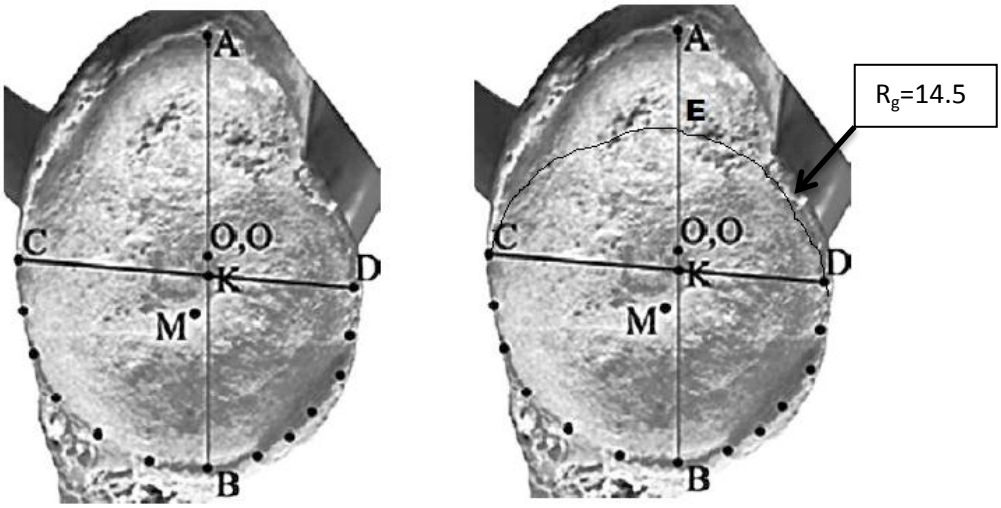

Figure 6. The glenoid geometry where A-B describes the dimension of the superior-inferior and C-D describes the dimension of the anterior-posterior.[14]

The humerus cartilage is thicker at the center and thinner at the periphery of the humerus.[68] Whereas, it is opposite for glenoid, which is thinner at the center (bare spot) and thicker at the periphery, as explained by Soslowsky et al.[41, 58] The thickness at the center of the humerus cartilage is 2.03 mm and for that of glenoid is 1.14 mm.[20, 58] All the selected values were considered from the data available on the male model. We chose to select the male gender for our study because most of the recurrent dislocation problems have been found in the male population as described by Owens et al.[47, 48] Pearl et al. contributed in describing the humeral shaft angle (HSA), which is 40.7º ± 4.7º as shown in the Figure 7 below[49]. The same results have been shown by some other researchers like Iannotti, who showed the neck shaft angle to be 134.7º.[29, 49] The right Figure shows the assembled view of the glenohumeral joint with humerus at 40.7º abduction.

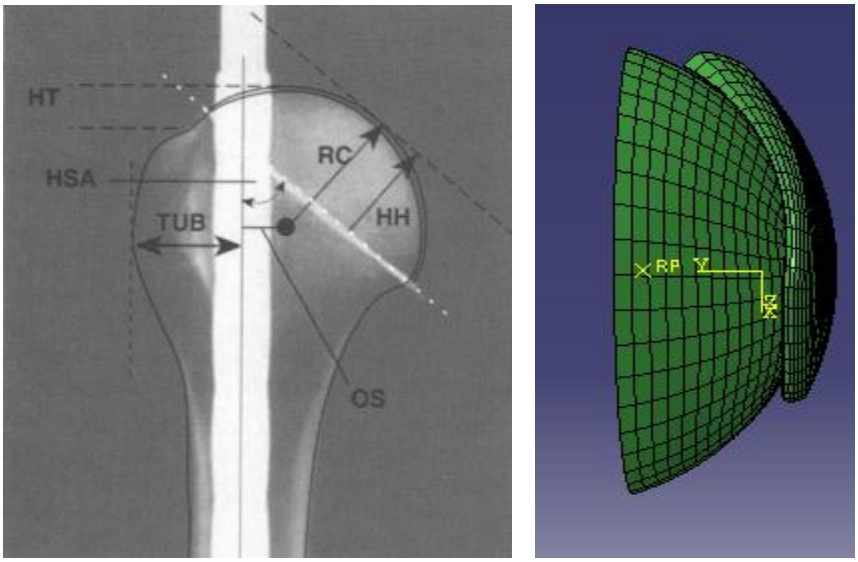

Figure 7. Humeral Shaft angle (HSA), whose average value is 40.7 degree, and on right is the assembly view of the glenohumeral joint.[49]

The glenohumeral joint and scapulothoracic joint move relative to one another, the ratio of movement of the glenohumeral joint to the scapulothoracic joint is 2:1.[16] It means that if the arm has to abduct at an angle of 90º then the humerus rotate at an angle of 60º but the scapula will rotate at an angle of 30º, the Figure 8 explains this.[27]

30 degrees of glenohumeral abduction = 45 degrees of arm abduction

60 degrees of glenohumeral abduction = 90 degrees of arm abduction

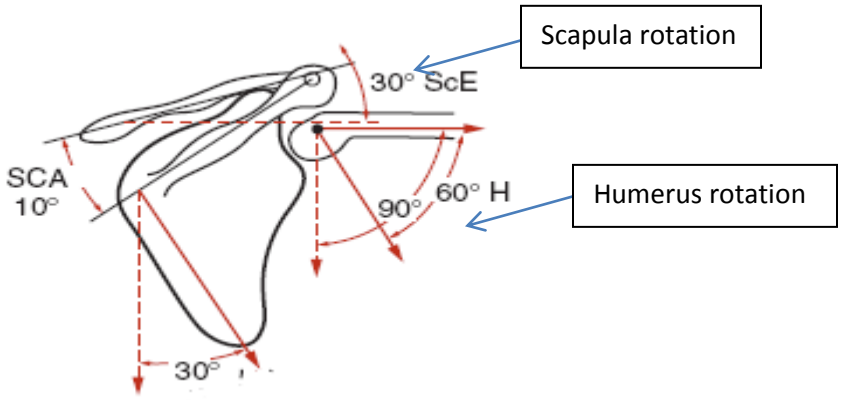

Figure 8. Detailed description of the Scapula and the Humerus abduction.[1]

1.3 Instability of shoulder joint

The stability of a joint is important for joint function. Similarly the stability of the glenohumeral joint is important for our body. Different ligaments, muscles, tendons, and other components of the glenohumeral joint play an important role in the stability of the shoulder. As described by Lippitt et al., the concavity compression effect helps to improve the stability.[38] This effect can be explained as when the convex humeral head

exerts pressure centered towards the concave glenoid; the concavity of the glenoid increases, hence, producing a stabilizing effect. The labrum at the glenoid fossa also has an advantage in the stability of the joint, as it increases the depth of the glenoid concavity and also increases the surface area of contact.[24, 30, 37] The stability of the glenohumeral joint is also improved by different stabilizers, i.e. static and dynamic stabilizers. The glenohumeral ligaments which are one of the stabilizers play an important role in the glenohumeral stability. The functions of the ligaments have been explained by Turkel et al., who suggested that the shoulder at 0º abduction maintains stability due to the subscapularis muscle; at 45º abduction the subscapularis, middle glenohumeral ligament and the anterosuperior fibers of the inferior glenohumeral ligament provide stability. At about 90º of abduction during the external rotation of the shoulder, the inferior glenohumeral ligament prevents dislocation.[59, 60] The glenoid has a smaller surface area of contact as compared to that of humeral head, which also affects the stability.[37, 41, 59] One of the other factors for instability is the shallowness of the glenoid fossa. The glenohumeral joint's stability worsens with the occurrence of lesions in either of the humerus, the glenoid or the labrum, which increases the probability of anterior dislocation.[52, 53]

The other reason found responsible for the anterior dislocation and instability of the shoulder is laxity of the ligaments and the rotarcuff.[52, 53] Rowe et al have put a lot of effort into explaining defects like the Bony Bankart lesion and the Hill-Sachs lesion; these lesions contribute to the anterior dislocation of the shoulder.[10, 53] Both the defects are shown below in the Figure 9. Furthermore it has been explained that, due to the repeated injury in the glenohumeral joint, a person can become more susceptible to

recurrent dislocations. This may limit the movement of the shoulder to a greater extent.[5, 52, 53] As explained earlier, the defect in the humeral head with erosion of cartilage and bony surface against the glenoid rim is known as the Hill Sachs defect, and the defect in the glenoid with loss of bone and detachment of the labrum is known as Bony Bankart lesion.[5, 10, 56, 64] With the Hill Sachs lesion, the convexity of the humeral head is lost and thus the humeral head is not able to compress the concave glenoid to achieve the concavity compression effect for stabilizing the glenohumeral joint.[38, 56] Rowe et al. explained that the most common reason for the recurrent dislocation and subluxation of the shoulder is the Bony Bankart lesion; also the excessive laxity of the capsule contributed to instability. The Hill Sachs defect was another important factor for the recurrent dislocation of the shoulder found by their group.[52, 53] Many authors have tried to explain through cadaveric studies that a single defect in either the glenoid or the humeral head will lead to a decrease in the stability ratio of the glenohumeral joint and the distance to dislocation decreases with an increase in the size of the defect.[27, 32, 56] A recent study by Wadjaja et al. stressed the anterior dislocation of the shoulder by correlating the presence of both the Bony Bankart and Hill Sachs lesion.[64] They did a statistical study for 61 patients between the years of 2003 and 2005, and concluded that when a Hill Sachs lesion is found in a plain radiograph, it can be useful in the prediction of the Bony Bankart lesion. Both these lesions are causes of the anterior dislocation in the shoulder.[64] Chaipat et al. also showed through the magnetic resonance imaging technique that the traumatic anterior dislocation can result in the tearing of the anterior inferior labrum and even loss of the bony structure from the anterior inferior portion of the glenoid rim.[11]

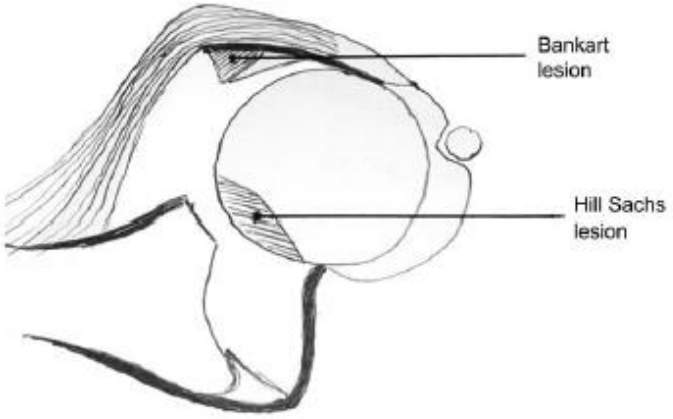

Figure 9. Dislocated shoulder with Hill Sachs lesion and Bony Bankart lesion.[64]

1.4 Significance of FEA in biomechanics

Finite element analysis (FEA) has been an important tool in the field of biomechanics and orthopedics. It has many useful applications for researchers, in particular the study of joint mechanics, tissue modeling and prosthetic engineering. The flexibility, smaller work, and lower cost for the FEA have led to its popularity in the field in the Biomechanics. With the advancement of the computing technology, FEA also have seen a widespread in the bioengineering industry. Richmond et al. took an effort to explain that FEA has derived from the mathematical models made in the past.[51] FEA software uses a numerical method solver based on applications and mathematical models made in the past. This type of computational analysis has many advantages over testing models mechanically. Mechanical testing requires more time and investment as lot of cost is involved with animal study and human specimens. The testing of specimens

requires separate fixture and equipment, adding to the cost and time associated with a particular experiment.

The flexibility of the FEA allows the user to perform experiment under different conditions and with multiple material properties. FEA is used to test the interaction between bone and prosthesis, understand joint motion mechanics, stress and strain calculation for tissues and tendon.[25, 50, 66] A contribution of FEA is in the area of pre-clinical testing of the implant device for interaction with the body, which allows researchers to obtain knowledge about the biomechanics of the musculoskeletal joints and research about tissue mechanisms, mechanics, growth and degeneration.[50] One of the biggest advantages of FEA is that patient specific model can be generated from the MRI and CT images and the material properties are selected accordingly from the previous literature data. From the images we can get the exact dimensions about geometry of the specimen of interest. The patient specific modeling will help to improve surgery outcomes. The analysis can be done non-invasively to know the characteristics of the bone prosthesis to be implanted before the operation. The analysis process using the FEA can be computed in much less time depending on the complexity and simulations can be performed at any number of iterations desired by the user.

Previous studies of finite element model of the glenohumeral joint have tried to analyze the effects of the glenohumeral capsule and ligaments on the stability of the shoulder but no study have looked at the bone defects in the glenohumeral joint.[15, 18, 23] Some studies analyzed the kinematics of the glenohumeral joint after the total shoulder arthroplasty. There are many studies which have analyzed the finite element model for the glenohumeral capsule since it contributes more towards the stability of the shoulder.[9,

[23, 45, 69] The bone defects also contribute a lot to instability, larger the bone defect more unstable the shoulder becomes. The larger bone defects have been found to affect the glenohumeral capsule as it gets lax due to the recurrent dislocation of the shoulder. For our study we chose to analyze the effects of isolated and combined bone defects with the help of finite element modeling.

Once we have the 3-D geometry of the model or design with few assumptions about the boundary conditions. For mathematical model we will make the free body diagram and make assumptions about the geometry, which may be different from the actual case. FEA also allows us to understand the nature of the forces, their magnitude, and material deformation occurring throughout the body. In additional to all of these computations, FEA goes beyond mechanical testing providing specific failure point data. Number of different variables can be computed by running one simulation from the field and history outputs.

1.5 Relevance-Aims and need of study

With the rise in the number of problems of dislocations, the shoulder's instability among the athletes and the general population is an important topic to be addressed. This has been a major topic of interest among researchers as clear knowledge about the glenohumeral joint's instability is not available. It is important to know how a particular kind of lesion with relation to the size of the lesion should be treated so that a person can return to the normal activity in his or her daily life. The cause of the defect can be a fall on the shoulder or trauma during aggressive activities like professional sports.

This study aims to explore the theoretical relationship between the interactions of the two major lesions in the glenohumeral joint of the shoulder.[17] The effects on the glenohumeral joint's stability related to different sizes of the Bony Bankart and the Hill Sachs lesions were studied at arm abduction angle of 45º and 90º. Then both the defects were tested simultaneously with different sets and a combination of the defect sizes. The result of the study will predict the stability ratio of the glenohumeral joint and the also the distance to dislocation will be reported depending on the different cases. The findings of the study will provide us with a clear picture about the shoulder's instability depending upon the nature and size of the defect. The study also tried to look how two smaller defects present at the same time in both the glenoid and the humerus effect the stability in comparison to the single larger defect. The results from which may have a clinical importance in understanding the importance of the different lesion with respect to their sizes. We hypothesize that as the size of the lesion increases, the glenohumeral joint's stability will decrease. We further hypothesize that the presence of both defects together will reduce the glenohumeral joint's stability to a greater extent than the presence of an individual defect.

CHAPTER II

METHODS

For the study we modeled three-dimensional glenohumeral joint components using the software package Rhinoceros 3D (Robert McNeel & Associates, Seattle, WA, USA) for geometry construction, which is a stand-alone, commercial NURBS-based 3-D modeling tool and TrueGrid (XYZ Scientific Applications, Inc, Livermore, CA, USA) for meshing of the geometry. A 3D hexahedral element mesh is generated for the glenoid and the humerus. The simulation of the joint loading and translation is performed using the FE software ABAQUS/6.9 Dassault Systèmes (Vélizy-Villacoublay, France). The study used static analysis for running simulations. The steps to draw the 3 D geometry and generate mesh for the model of the glenoid and the humeral head are explained below.

2.1 Generation of the geometry

The 3- dimensional model for glenoid and humerus were made using the software package Rhinoceros 3D and TrueGrid the steps for which are explained below:

2.1.1 Modeling the Glenoid

The model was made using Rhino. First start with the circle command and draw two circles. The first circle has a radius of 26.37 mm and the center at coordinates (0, 0), after that another circle of radius 34.5 mm is drawn at (0, 7.05) coordinates. The two lines are drawn one horizontal and another vertical intersecting each circle passing through coordinates (0, 0). Then the parts of the circle are trimmed so that arc is left only in the fourth quadrant as shown in Figure 10. Then a vertical axis is drawn so that both arcs can be revolved around that axis at an angle of 360º. Then on top of the hemisphere, a circle of 14.5 mm radius is drawn with center at (0, 0) coordinates. And a line of length 39 mm is drawn from one end of the circle. Then a spline is drawn passing through point (-14.5, 0); (0, 24.5) and (14.5, 0). After that we use the extrude cut command to get the desired shape of the glenoid, which looks similar to a pear. Then the model is saved in the form of iges file, so that it can be used in TrueGrid (XYZ Scientific Applications, Inc, Livermore, CA, USA) for meshing.

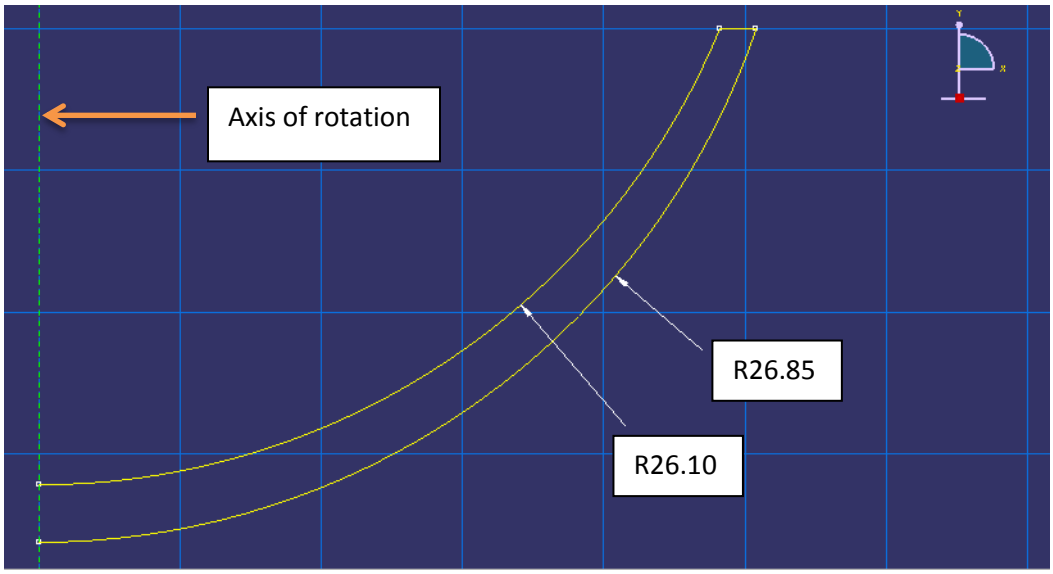

Figure 10. Revolution step to create geometry.

2.1.2 Modeling the humerus

The humerus was modeled using TrueGrid so that it can be modeled and meshed at the same time. First, a block was created and then in the block menu we used surface definition command to define the two surfaces for the circle. The center of the circle is at coordinates (0, 0, 0) and the radius is 26.10 mm. Then we draw another circle with center at coordinates (0, -1.28) and the radius of circle will be 26.85 mm. Then another surface definition is defined which will be a horizontal plane, the plane will cut the spheres into hemisphere which will look like the shape of the humeral head. These surfaces are used to mesh the model for the FEA simulations. The commands are given below:

block 1 8 16 23; 1 3; 1 8 16 23; 1 8 16 23; 1 3; 1 8 16 23 } Creating a block

sd 1 sp 0 0 0 26.10

sd 2 sp 0 0 -1.28 26.85 } Defining surface definition

sd 3 plan 0 0 -10 0 0 1

2.2 Creation of mesh

Mesh creation is the important part of the computational biomechanics. If mesh is not created with proper selection of the element, mesh density, size of the element, and proper element orientation along the thickness, the results of the study can vary by large value and may affect the sensitivity analysis. For meshing the model we used hybrid 3D hexahedral elements (C3D8H). These element type has 8 nodes and 6 quadrilateral faces. Using hexahedral mesh than tetrahedron will result in lesser number of elements. The advantages of the hexahedral element are regularity, proper angle distribution and anisotropy.[55] Even the tetrahedral quadratic type element provide good results in some of

the structural problems, but the results of hexahedral elements are much better than the tetrahedral element. The hexahedral element shows better convergence and sensitivity results to the mesh orientation.[55] The reaction of hexahedral elements to the application of body loads will more precisely corresponds to loads similar to real world conditions.

2.2.1 Steps for generating the glenoid mesh

Using TrueGrid we created a block and imported the iges file of the model. A butterfly mesh was created by removing certain portion at the edges of the block and defining the block boundaries for a butterfly mesh. We used the block boundary command for all the edges and 4 block boundaries were defined. The reason we created a butterfly block is that, it is it takes the exact shape of the surface on which it is projected, being uniform all around the surface. It is useful where two surface have a contact and smooth translation is required. The next step was to move the mesh block close to the geometry of the glenoid. After this the faces and edges of the block were projected and attached respectively to the geometry using the projection and the attach command. Then we did surface and volumetric smoothing of the mesh using unifm command. Figure 11 below shows the meshed model of glenoid. The commands are shown below:

block 1 6 11 16; 1 6; 1 6 11 16; 1 6 11 16; 1 6; 1 6 11 16; } creating a block

iges C:\users\piyush\desktop\newglenoid.igs 1 1 } importing the model

dei 1 2 0 3 4; 1 2; 1 2 0 3 4; } deleting the corners of block for butterfly block

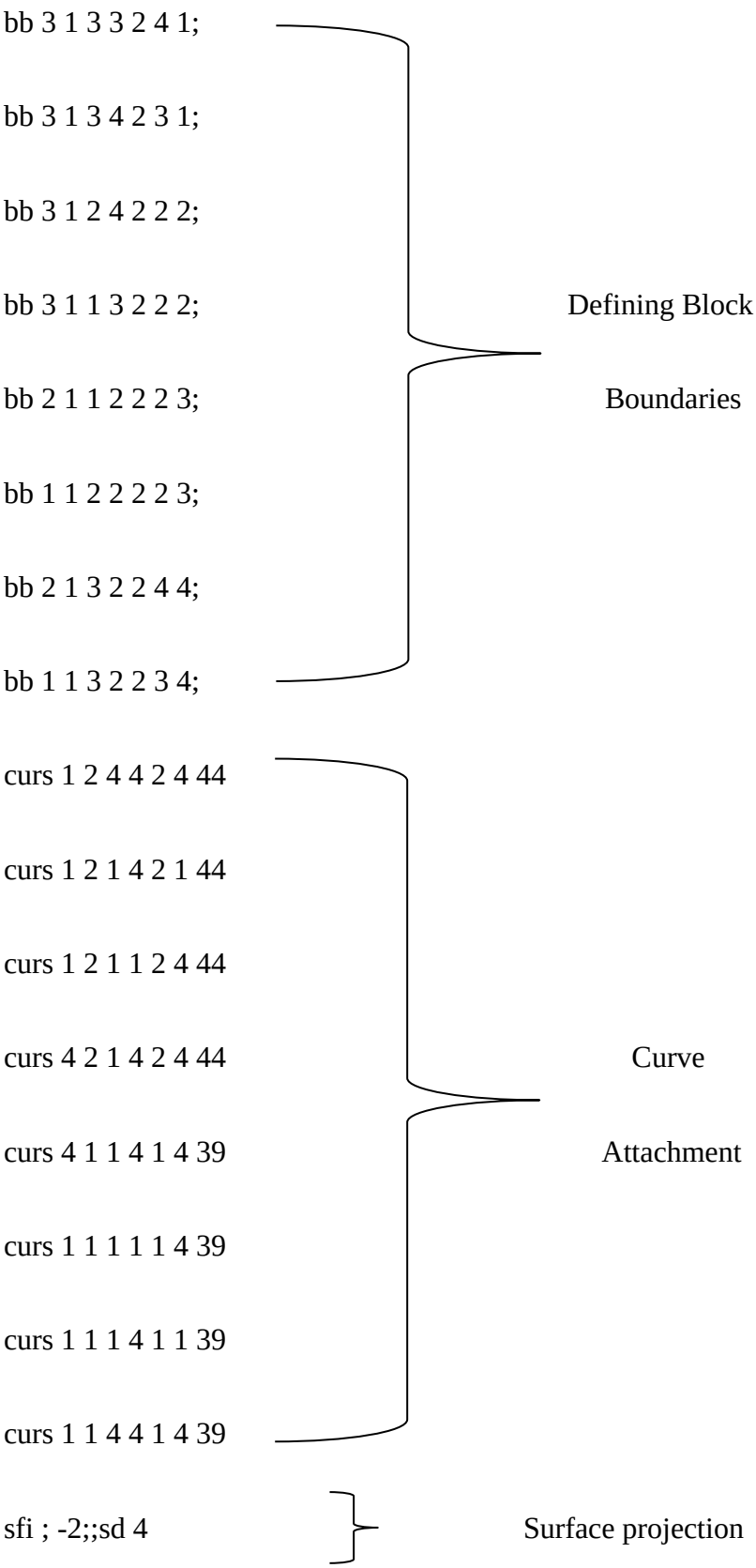
bb 3 1 3 3 2 4 1;
bb 3 1 3 4 2 3 1;
bb 3 1 2 4 2 2 2;
bb 3 1 1 3 2 2 2;
Defining Block
bb 2 1 1 2 2 2 3;
Boundaries
bb 1 1 2 2 2 2 3;
bb 2 1 3 2 2 4 4;
bb 1 1 3 2 2 3 4;
curs 1 2 4 4 2 4 44
curs 1 2 1 4 2 1 44
curs 1 2 1 1 2 4 44
curs 4 2 1 4 2 4 44
Curve
curs 4 1 1 4 1 4 39
Attachment
curs 1 1 1 1 1 4 39
curs 1 1 1 4 1 1 39
curs 1 1 4 4 1 4 39
sfi ; -2;;sd 4
Surface projection

sfi ; -1;;sd 5

sfi ;; -1 0 -4;sd 100 } Surface Projection

sfi -1 0 -4;;;sd 100

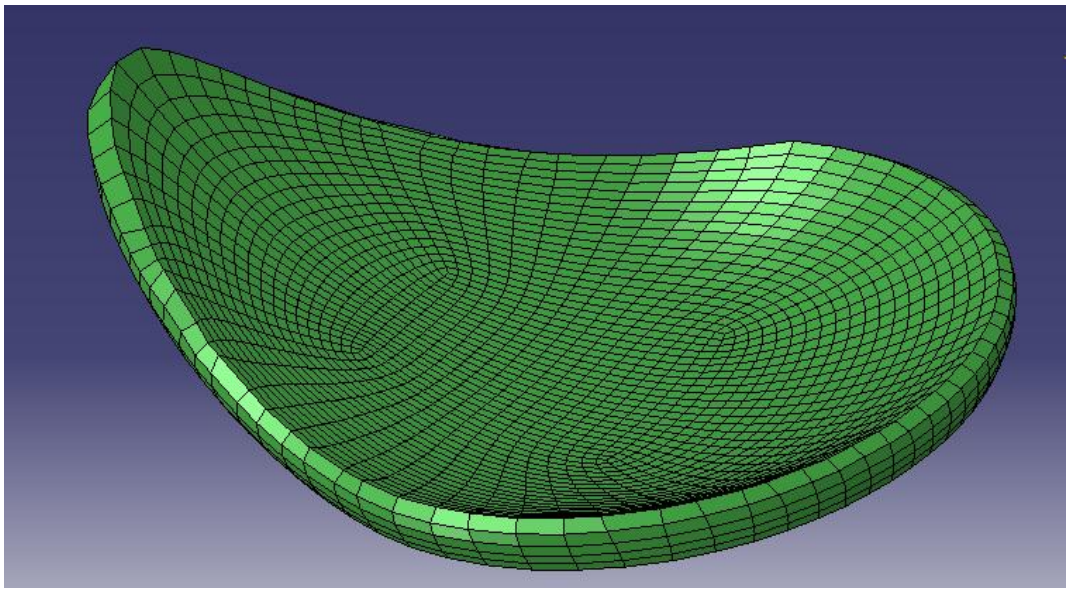

Figure 11. Glenoid geometry and mesh

2.2.2 Steps for generating humeral head mesh

Using the surfaces created in the previous section 2.1.2, we mesh the geometry for the humeral head with help of TrueGrid using butterfly mesh as shown in Figure 12. Then the faces of the butterfly block are projected on to all the surfaces. At the end the unifm command is used to do surface and volumetric smoothing. The commands used for this are shown below:

block 1 8 16 23; 1 3; 1 8 16 23; 1 8 16 23; 1 3; 1 8 16 23 } Block Creation

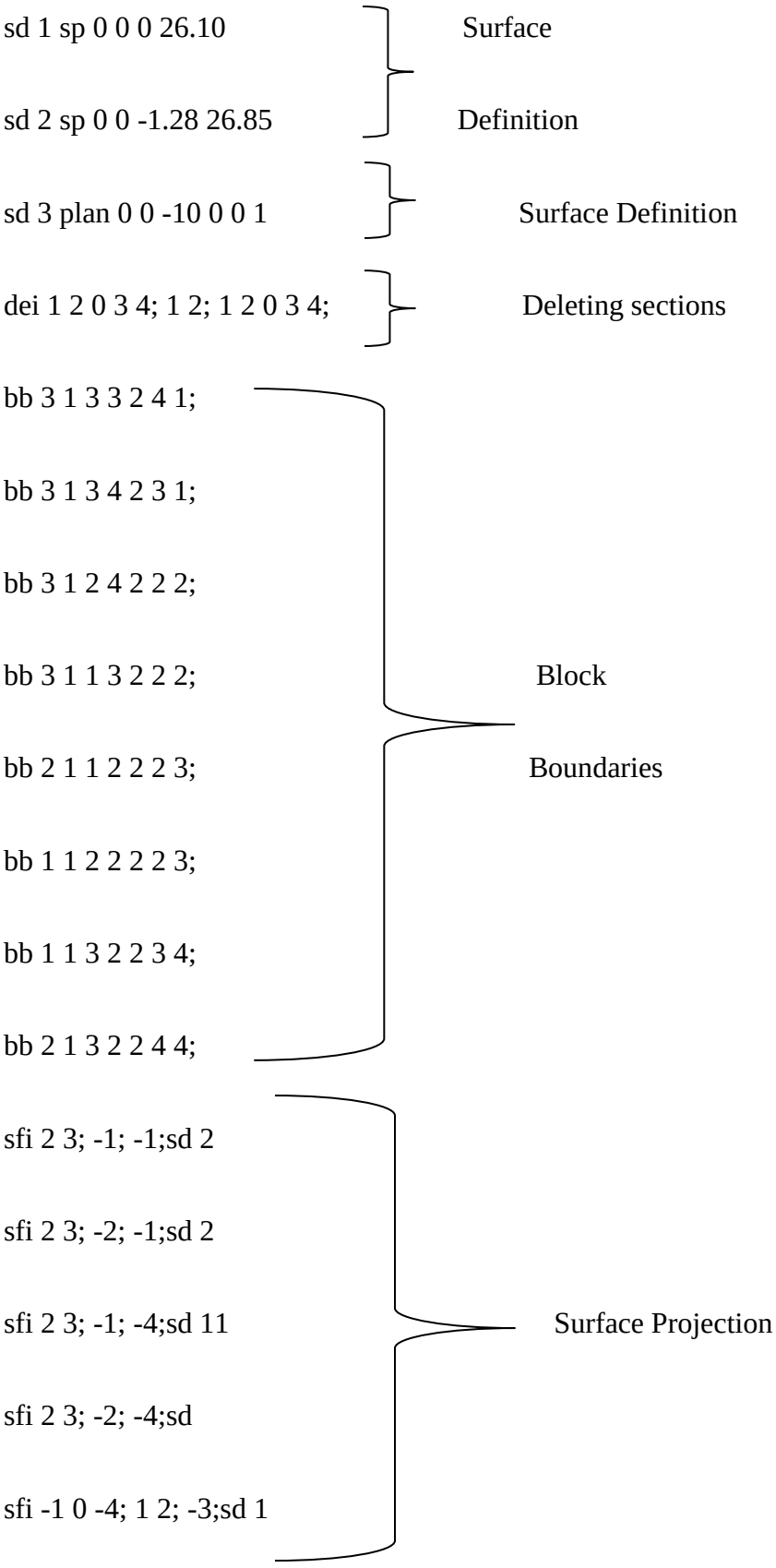
sd 1 sp 0 0 0 26.10
Surface
sd 2 sp 0 0 -1.28 26.85
Definition
sd 3 plan 0 0 -10 0 0 1
Surface Definition
dei 1 2 0 3 4; 1 2; 1 2 0 3 4;
Deleting sections
bb 3 1 3 3 2 4 1;
bb 3 1 3 4 2 3 1;
bb 3 1 2 4 2 2 2;
bb 3 1 1 3 2 2 2;
Block
bb 2 1 1 2 2 2 3;
Boundaries
bb 1 1 2 2 2 2 3;
bb 1 1 3 2 2 3 4;
bb 2 1 3 2 2 4 4;
sfi 2 3; -1; -1;sd 2
sfi 2 3; -2; -1;sd 2
sfi 2 3; -1; -4;sd 11
Surface Projection
sfi 2 3; -2; -4;sd
sfi -1 0 -4; 1 2; -3;sd 1

sfi -1 0 -4; 1 2; -2;sd 2

sfi -1 0 -4;;;sd 3 — Surface Projection

sfi ;; -1 0 -4;sd 3

unifm 2 1 1 3 1 4 & 1 1 2 2 1 3 & 3 1 2 4 1 3 & 2 2 1 3 2 4 & 1 2 2 2 2 3 & 3 2 2 4 2 3 & 2 1 1 3 2 1 & 2 1 4 3 2 4 & 1 1 2 1 2 3 & 4 1 2 4 2 3 40 0 1 — Surface and vol. Smoothing

unifm 2 1 1 3 2 4 & 1 1 2 2 2 3 & 3 1 2 4 2 3 60 0 1

merge

stp .00001

abaqus write — Generating Abaqus input file for model

info

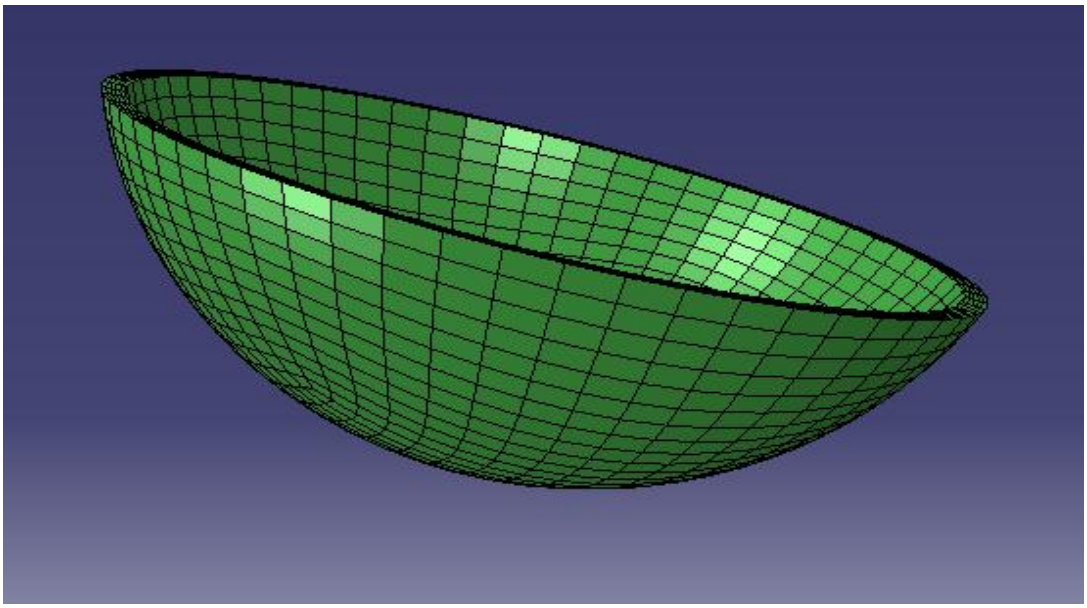

Figure 12. Humerus meshed geometry.

2.3 Material property definitions

After all the components were meshed in TrueGrid, the models were imported into Abaqus. Then we define the material properties for the cartilage as Neo-Hookean hyperelastic, incompressible material. As taken from a previous study by Buchler and Iannotti et al we selected the young's modulus (E) to be 10 MPa and the Poisson's ratio (ν) to be 0.4.[4, 9, 21] We calculated the constants for material properties for hyper-elastic material using the equations 1 and 2 given below. The value of D_{10} constant to be used for the Abaqus can be derived from equation 3 given below. The Table 1 shows values for the constants. After the material property has been defined, we establish different section definition for humerus and glenoid cartilage. Then we define the section property by selecting the elements of the humerus and the glenoid.

$$C_{10} = \frac{E}{4(1+\nu)} \tag{1}$$

$$D_{10} = \frac{E}{6(1-2\nu)} \tag{2}$$

$$D_{10}' = \frac{1}{D10} \tag{3}$$

Table 1. Values of the material constants.

Constants	Values
C_{10}	1.79
D_{10}	8.33
D_{10}'	0.12

2.4 Steps for the assembly of the model

The two rigid body points are created using Abaqus, one point at coordinates (0, 0) and other at coordinates (0, -40). These rigid body points are considered as rigid bone for the humerus and glenoid. After that all the four instances are added in the assembly mode. First, we added both the rigid points, and then we added the glenoid instance to the assembly mode. The glenoid instance is rotated about the Y-axis at an angle of -135º so that it anterior inferior position of the shoulder is the positive X-direction, after that the instance is translated 3 mm in negative Y direction. The second instance, humerus is added to the assembly database. Then the instance is rotated about X axis at an angle of -90º. And to obtain the 90º abduction we rotate it by -19.3º about the axis 1, 0, -1. The assembled view of the joint is shown in Figure 13.

30 degrees of glenohumeral abduction = 45 degrees of arm abduction

60 degrees of glenohumeral abduction = 90 degrees of arm abduction

To achieve 90º arm abduction, we subtract the humerus shaft angle from the glenohumeral abduction (60º - 40.7º = 19.3º).

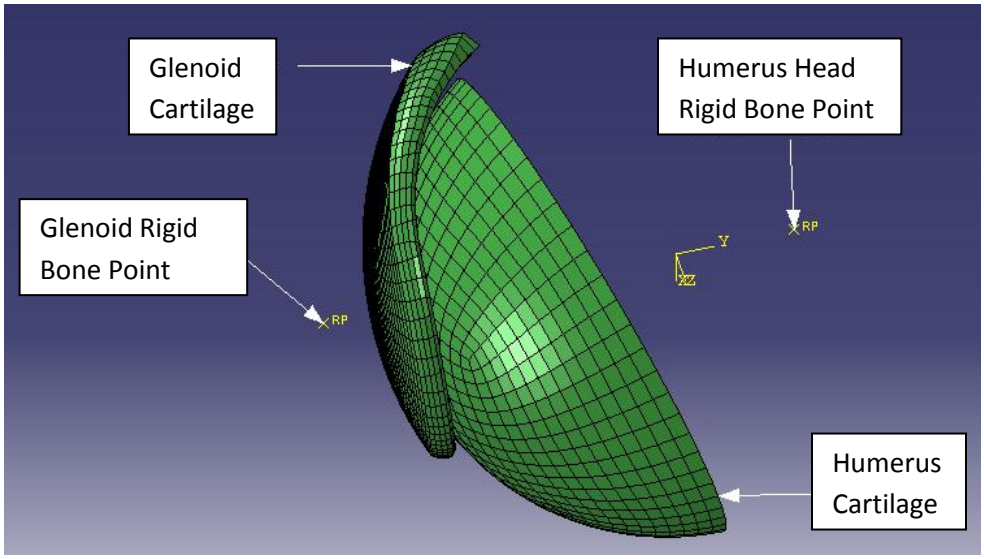

Figure 13. Different components of the glenohumeral joint and their assembly

2.5 Interaction properties

The interaction between the two cartilages is defined using node to surface contact. The humerus cartilage is considered as the master surface and the glenoid is selected as the slave surface. The property of the surface contact is defined to be tangential with frictionless contact and mechanical hard contact with normal behavior, which uses the Augmented Lagrange enforcement method. A study by Anderson et al. described the use of Augmented Lagrange method to enforce incompressibility.[4] The humerus bone rigid point is constrained to the humeral head cartilage using a coupling. Similarly the glenoid rigid bone point is also constrained using coupling to the glenoid cartilage. Figure 14 shows the interaction properties between components.

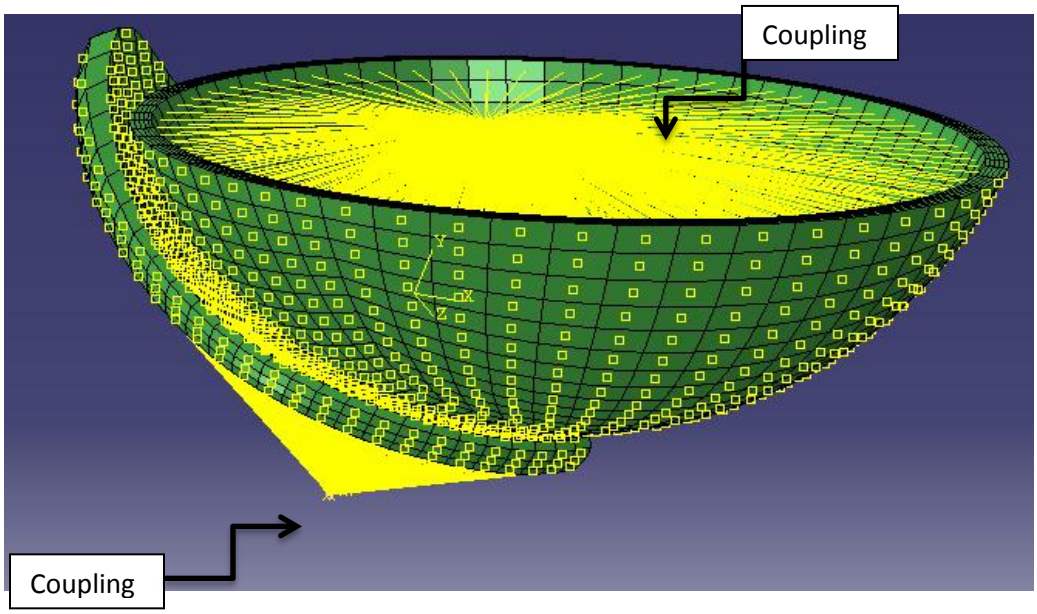

Figure 14. Surface contact and constraints for the joint.

2.6 Setting up different steps for simulation

In the step module we create different steps for simulating our experiment. Three steps were defined for the whole simulation. Different steps are known as Contact, Loading, and Translation. In the contact step the humerus cartilage comes in contact with the glenoid cartilage. At the loading step a compressive force of 50 N is applied at the humerus rigid body directed towards the lateral side of the shoulder. In the final step the humerus translates in the X direction i.e. the anterior inferior position of the shoulder. The analysis is a static type and displacement controlled to mimic the cadaveric study done by Kaar et al.[32]

2.7 Setting up the load and boundary conditions

The compressive force of 50N is applied on the humeral head until the shoulder dislocates. Same procedure is repeated for all different conditions of the defect. We chose

to select 50 N compressive force, because it has been reported to be nominal force need for the shoulder to dislocate and it has been used in many shoulder studies as a standardized force. Both the studies which we used for validation of our model used the same compressive axial force.[27, 32] Certain boundary conditions are set for experimental setup, as explained. The glenoid cartilage and the glenoid rigid bone point are turned into one set, which was labeled "glenoid" and the glenoid bone point is encasterd to restrict movement in all directions for all the steps. Then the second rigid body part and the humeral head cartilage are also made as one set labeled as "humerus". The boundary condition for the humeral head bone point is set different for individual step. In the beginning, during contact step, the humerus set moves 1.2 mm in lateral direction (y-direction) to make a contact with the glenoid surface, and all remaining movements are constrained. Then in the next step, which is load step the humerus set is left free to translate in Y direction but all other movements and rotations are constrained. The boundary condition for the last step is, the humerus set is allowed to move freely in Y direction and is translated specific distance in anterior inferior direction (X-direction) to nearly 17 mm.

2.8 Selection of variable for output

For the study variables of interest for the output are displacements and reaction forces. We select variables of interest from the history output for both sets of the glenoid and the humerus. The entire variable selections can be plotted individually to interpret the result.

2.9 Mesh convergence analysis

For selecting the appropriate mesh we ran a mesh convergence study with different number of elements for the whole model and different number of elements across the thickness. To find the converging point for the mesh study we compared changes in values of peak reaction force with respect to the number of elements in the model, but the changes were negligible. Then to find the converging point for the mesh study we compared changes in the maximum values of von Mises stress with respect to the number of elements in the model. Then selection is made for the mesh based on the results from the study as shown in the chapter 3.

2.10 Creating defects in the humerus and the glenoid

The defects are created using a plane to cut the area of the bone loss defect. This is done using the TrueGrid software, in the block interface we define a place as a surface and one of the faces of the butterfly block is projected on to the surface. And smoothing is done for the surface and volume of the block. Four individual defects are made in both humerus and glenoid. The size of the defects is selected similar to the ones from previous study done by Kaar et al. and Itoi et al.[27, 32] Then we combine both sets of the defects and run the simulations for the arm abduction of 45º and 90º.

For creating the defect in the glenoid we used the same method used by Itoi et al. for different sizes of the defects.[27] The defects were created with respect to radius of the glenoid, we chose 4 sizes of the defect which are ¼*R_g, ½*R_g, ¾*R_g and 1*R_g. As shown in Figure 6 above the radius, R_g for the glenoid is 14.5 mm. The osteotomy lines for the defects are shown in the Figure 15 below. The osteotomy lines 1, 2, 3 and 4 represents the plane for the defects ¼*R_g, ½*R_g, ¾*R_g and 1*R_g respectively.

The humeral head defects were created for four different sizes. They were made similar to the study done by Kaar et al.[32] The sizes of the defects were selected as 1/8*R_h, 3/8*R_h, 5/8*R_h and 7/8*R_h. the radius R_h of the humerus is 26.85 mm. The osteotomy lines for the defects of the humerus are shown in the Figure 15 below. The lines 1, 2, 3 and 4 are the osteotomy lines for the defect size 1/8*R_h, 3/8*R_h, 5/8*R_h and 7/8*R_h. Table 2 describes the value of the size of the defects.

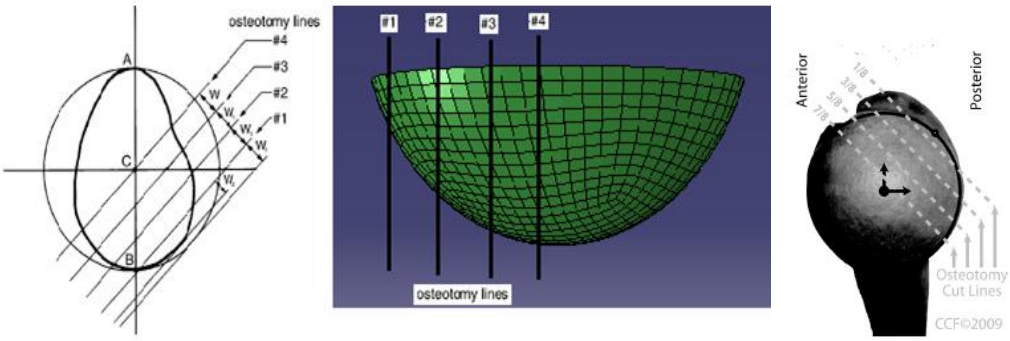

Figure 15. Osteotomy lines for the defects of Glenoid on left and humerus on right.[27, 32]

Table 2. Size of defects for the glenoid and the humerus.

Osteotomy Lines	Width of Glenoid defect	Width of Humerus defect
1	3.63 mm (1/4* R_g)	3.36 mm (1/8* R_h)
2	7.25 mm (1/2* R_g)	10.06 mm (3/8* R_h)
3	10.89 mm (3/4* R_g)	16.78 mm (5/8* R_h)
4	14.5 mm (R_g)	23.49 mm (7/8* R_h)

2.11 Calculation of the stability ratio

For the calculation of the stability ratio we need to calculate the net peak reaction force acting on the humerus. The peak reaction force in the x-direction is Fx acting opposite to the direction of the translation motion of the as shown in Figure 16. The force in the y-direction is our compressive force acting on the humerus, which is constant throughout the motion. Fx will tend to oppose the motion of the humerus to prevent it from dislocating from glenoid. So the net stabilizing force (RHF) acting on the humerus will be Fx. This force will try to stabilize the humerus motion of translation.

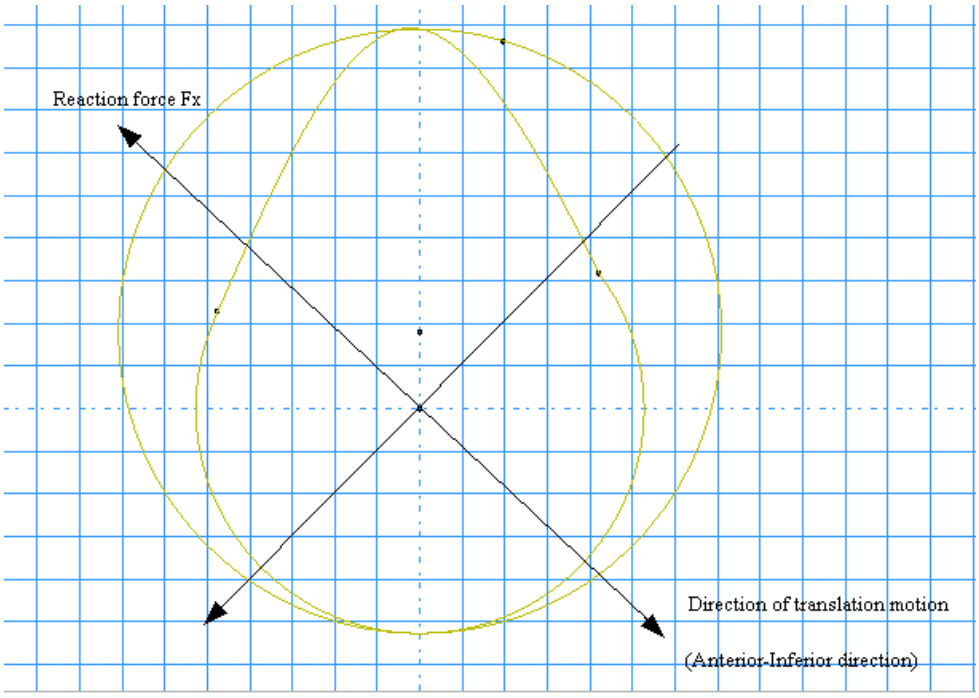

Figure 16. Reaction forces acting on the humerus, when humerus translates in anterior inferior direction (x-direction).

The stability ratio is calculated using the equation 4 given below. It is expressed as the ratio of Net reaction force on humerus (RFH) to the compressive load acting on the shoulder. Two studies by Itoi et al. group show that they also looked the reaction force in the direction of the translational motion of the humerus.[27, 67]

$$Stability\ Ratio = \frac{Net\ reaction\ forces\ (RFH)}{Compressive\ force} \quad (4)$$

2.12 Determining the point of dislocation

The dislocation point is the point at which the humeral head comes off the glenoid. The distance traveled by the humeral head during translation step from the initial point until the point of dislocation is called the distance to dislocation. The graphs were plotted with the data sets of distance of the humerus in anterior direction on horizontal axis of the graph and distance of the humerus in lateral direction on vertical axis of the graph. Then we pick the maximum value on the y-axis, corresponding to that point x value was selected. The corresponding point on the x-axis is the point of dislocation and distance from zero till that point defines the distance to dislocation as shown in Figure 17 below. The instability occurs in the shoulder after multiple dislocations, which makes the shoulder prone to recurrent dislocation.

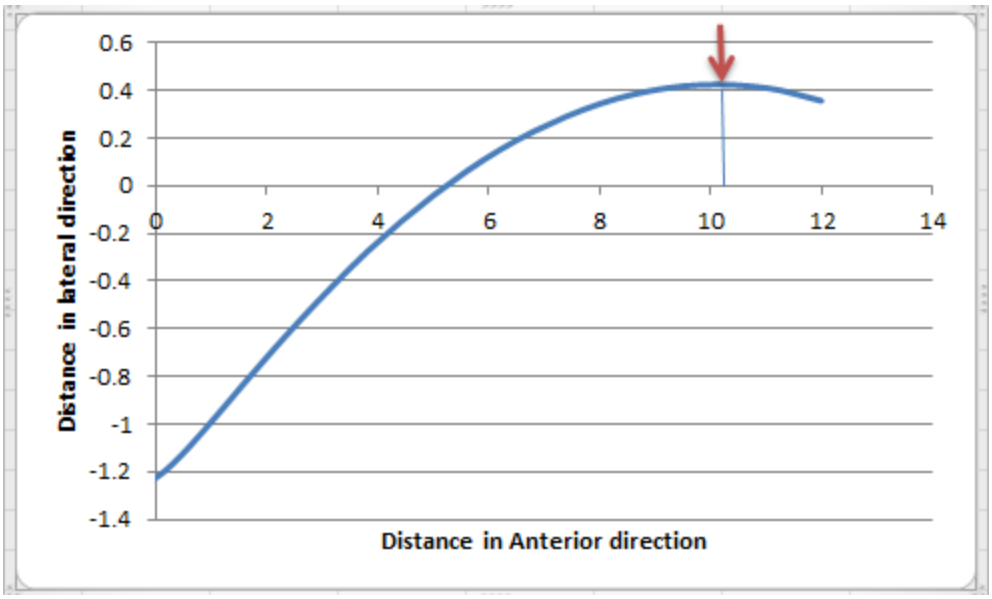

Figure 17. How to determine the point of dislocation

It can be seen from the Figure 16 that the distance to dislocation is 10.3 mm.

2.13 Different positions of the glenohumeral joint

The experimental protocol includes two arm positions, i.e. 45º and 90º abduction and neutral rotation. So we run all simulations for different combinations of defects at both 45º and 90º abduction considering the arm to be in neutral rotation. The Figure 18 below shows the position of the shoulder with abduction angles 45º and 90º.

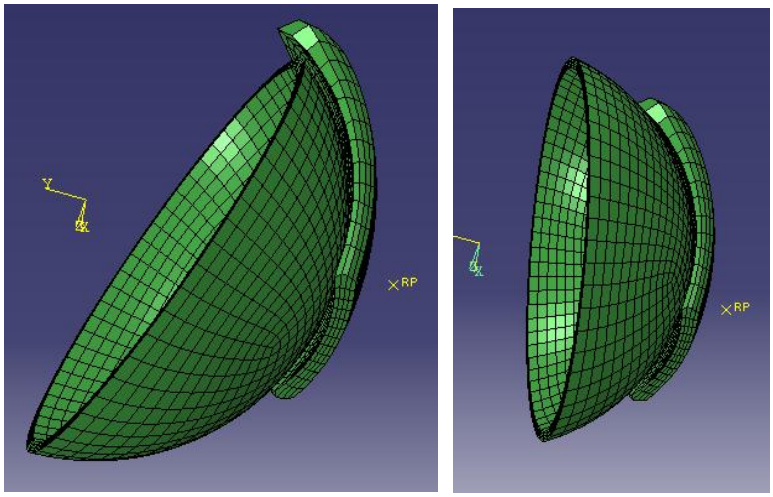

Figure 18. The shoulder at 90° and 45° abduction respectively

Some extreme positions of combined defects with the large defect in the glenoid and the humerus are shown in the Figure 19. It can be seen that the arm above 45º abduction angle, cannot maintains it stability, as it dislocates completely for the larger defects at higher abduction angles. The Figure 19 below shows the two case at 90º abduction, with the largest glenoid defect (R) and the humerus defect 7/8 *R and second one is largest humerus defect (7/8*R) and the glenoid defect size 3 (3/4*R) respectively. In the first case, there is no contact between the two; but for the second case, the joint's stability fails as soon as the load is applied.

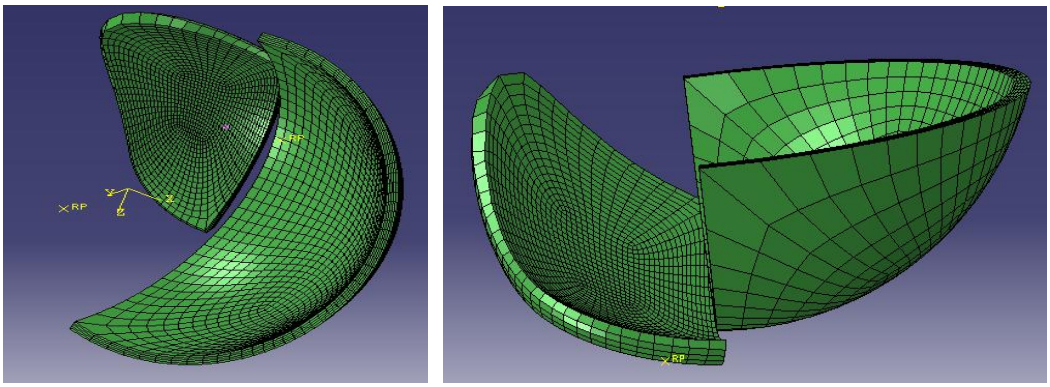

Figure 19. Extreme cases with the largest glenoid defect and the largest humerus defect respectively, which has zero stability

CHAPTER III

RESULTS

3.1 Mesh convergence study

Figure 20 shows the result from the convergence study done for our model. On the horizontal axis of the graph we plotted the number of elements and on the vertical axis max. von Mises stress was plotted. From the results we selected 5 elements across the thickness of the cartilage and about 7360 number of elements. This point is described as the point of convergence, as indicated by the downward red arrow on the Figure. After this point there is not much variation in values of the max. von. Mises stress it can be said that convergence is achieved. As mentioned earlier in section 2.9, the plot for reaction force vs. the number of elements had no significance variation with change in number of elements so we compared max. von Mises stress and number of elements.

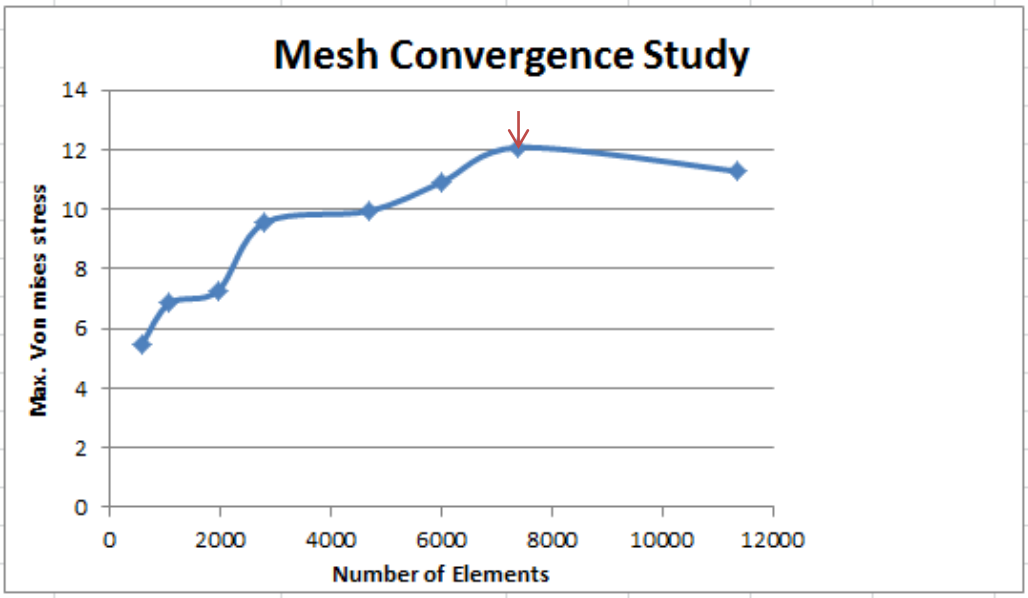

Figure 20. Point of convergence for the mesh study is shown by the arrow.

3.2 Reaction force

We recorded the reaction forces in x and z-direction from all the simulations. Their vector sum is described as peak reaction force, as described in section 2.11. This will help us to calculate the stability ratio of the joint. Table 3 shows the results for peak reaction force in x and z-direction for both the abduction angles.

Table 3. Peak reaction force acting on the humerus in x-direction

Reaction force in x-direction											
		Glenoid defects									
		Intact at 90°	Intact at 45°	1/4R at 90°	1/4R at 45°	1/2R at 90°	1/2R at 45°	3/4R at 90°	3/4R at 45 °	R at 90°	R at 45°
Humeral head defects	Intact	21.5	21.9	15.1	15.8	8.03	8.7	1.4	1.7	0	0
	1/8R	21.5	21.9	15.13	15.74	8.06	8.7	1.3	1.7	0	0
	3/8R	21.5	21.9	15.05	15.8	8	8.7	1.4	1.7	0	0
	5/8R	21.5	21.9	15.3	15.7	8.2	8.8	1.4	1.8	0	0
	7/8R	21.3	21.9	15.2	15.8	8.9	8.6	0	1.7	0	0

3.3 Isolated defects

The results for percentage of the intact translation of the isolated Hill Sachs defects are shown in the Figure 21 & 22 below, which are calculated with respect to the

intact joint translation. To calculate the percent translation we divided the value of translational distance for defects by the translational distance to dislocation for the intact joint. Figure 21 compares the percentage intact translation results from our study with results from the study by Kaar et al. at 90º abduction and neutral rotation of the arm, as a part of the validation process. The horizontal axis of the figure describes the size of the humeral head defect and the vertical axis shows the % intact translation of the humeral head till the point of dislocation. The comparison shows that the results for the 90° arm abduction has a same trend and nearly equal values for the percentage translation. The Figure 22 shows the results for the comparison of the results of our study and study by Kaar et al. at 45º abduction and neutral rotation of the arm.[32] The horizontal axis represents the size of the defects and vertical axis represents the % intact translation of the humerus, which is calculated with respect to the intact joint translation. It is seen that for all the first three smaller sizes of defects, the distance to dislocation is nearly same, being approximately 14 mm, but for the largest defect the distance to dislocation decreases approximately to 10 mm. At 45º abduction the results are slightly different, the distance to dislocation for an isolated Hill Sachs defects are same for the first three defects, being 14 mm but for the largest defect it reduced to 13.6 mm. The stability ratio of the glenohumeral joint did not vary for different sizes of the defect at 90º abduction and neutral rotation; it was nearly same for all the four cases as shown in Figure 23. The same pattern is seen for the test at 45º arm abduction and neutral rotation, but the stability of the joint for first three defects is approximately 1% greater for 45º arm abduction as compared to 90º arm abduction. At 90° abduction the humeral defects have stability ratio

nearly equal to 43%. For the 45° abduction, the stability was approximately 44% for the defects.

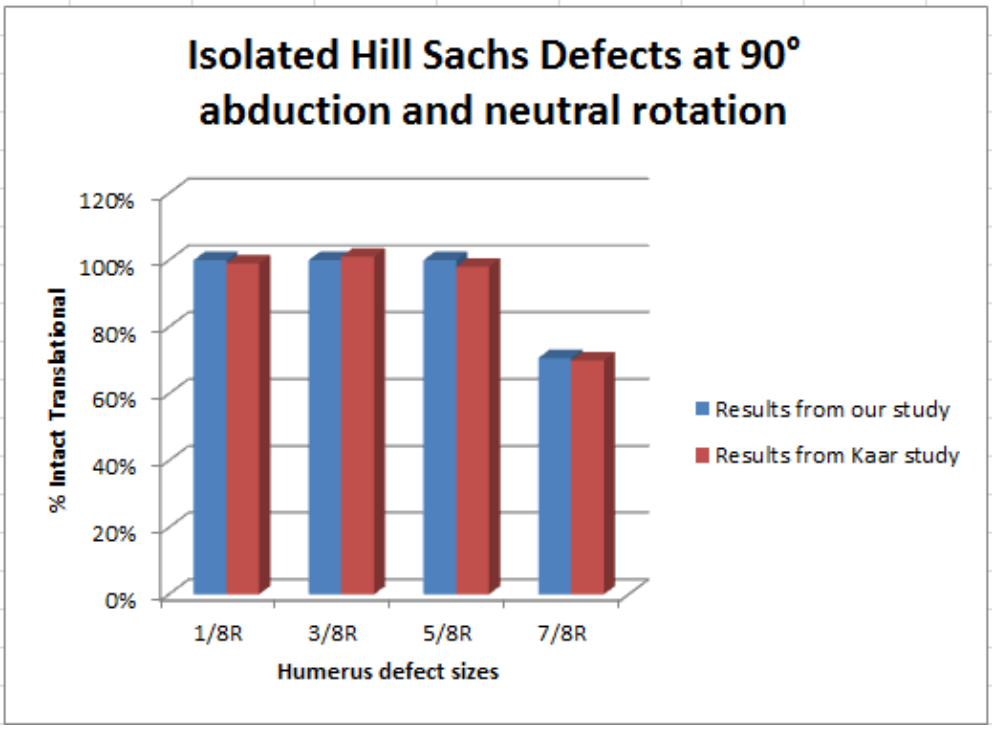

Figure 21. % intact translation for isolated Hill Sachs lesion at 90° abduction and neutral rotation, which is calculated with respect to the intact joint translational distance, compared to results from study by Kaar et al.[32]

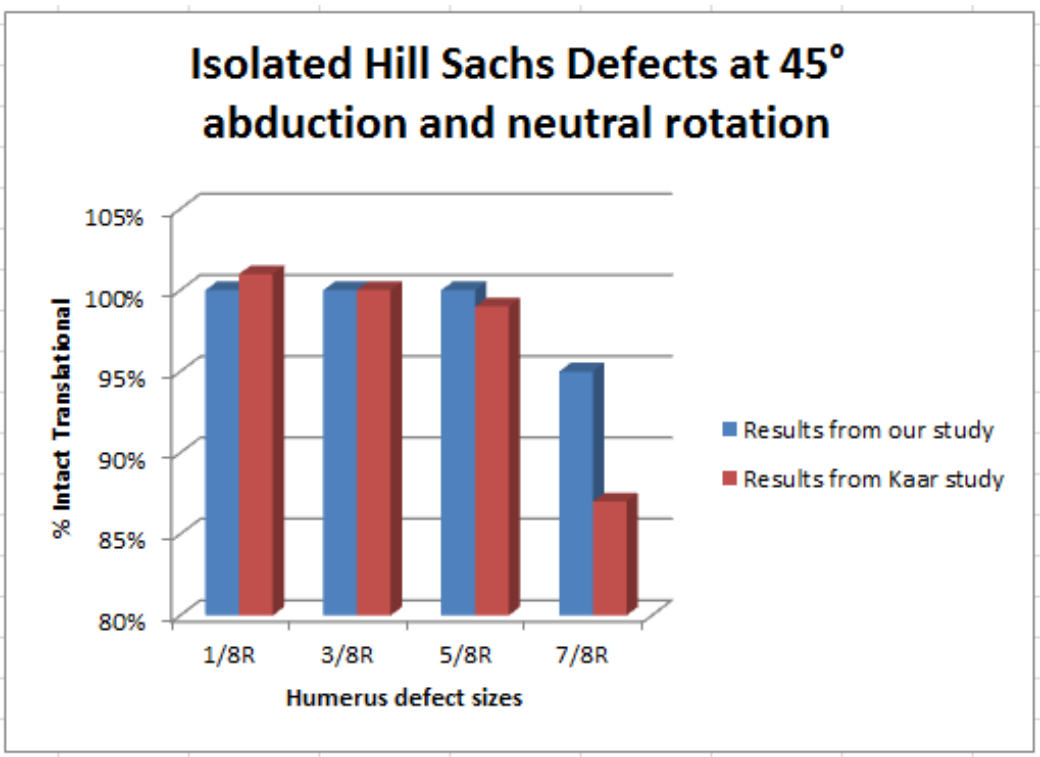

Figure 22. % intact translation for isolated Hill Sachs lesion at 45° abduction and neutral rotation, which is calculated with respect to the intact joint translational distance, compared to results from study by Kaar et al.[32]

In Figure 22, the x-axis represents the size of the defects and the size of defects increase from 1/8*R of the humerus to 1/8*R. The y-axis represents the % intact translation of the humerus, which is calculated with respect to the intact joint translation. We compare the results from our study with the results from the study by Kaar et al.[32] The horizontal axis of the Figure 23 describes the size of the humeral head defects and the vertical axis describes the stability ratio of the joint.

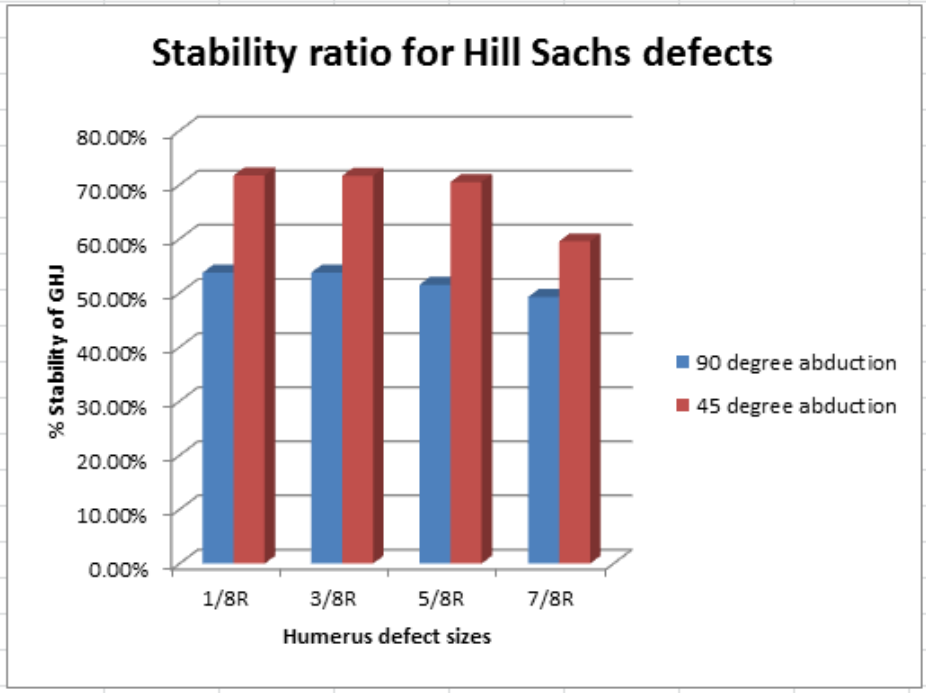

Figure 23. Stability ratio for the isolated Hill Sachs lesion for 90° and 45° abduction and neutral rotation of the arm.

The results for percentage of the intact translation for the isolated Bony Bankart defect at 45º and 90º abduction with neutral rotation of the arm are shown in the Figure 24 below. The horizontal axis of the figure shows the sizes of the glenoid defects and the vertical axis of the figure describes the % intact translation of the humerus. It can be seen clearly that the value for % intact translation decrease with the increase in the size of the defect. The values for the percentage intact translation in both the cases of abduction (45º and 90º) are approximately same for individual defect. The results of the net peak reaction force on humerus (RFH) from the study by Itoi et al. were compared with the results from our study.[27] The testing conditions for both the studies were nearly same, both tested at 90° abduction angle of the arm but the only difference was the rotation of arm; we tested different defect states at external, internal, and neutral rotation and Itoi et

al. tests included external and internal rotation of the arm. This comparison was done for validation of our model. The comparison of results for the peak reaction force, RFH can be seen in Figure 25.

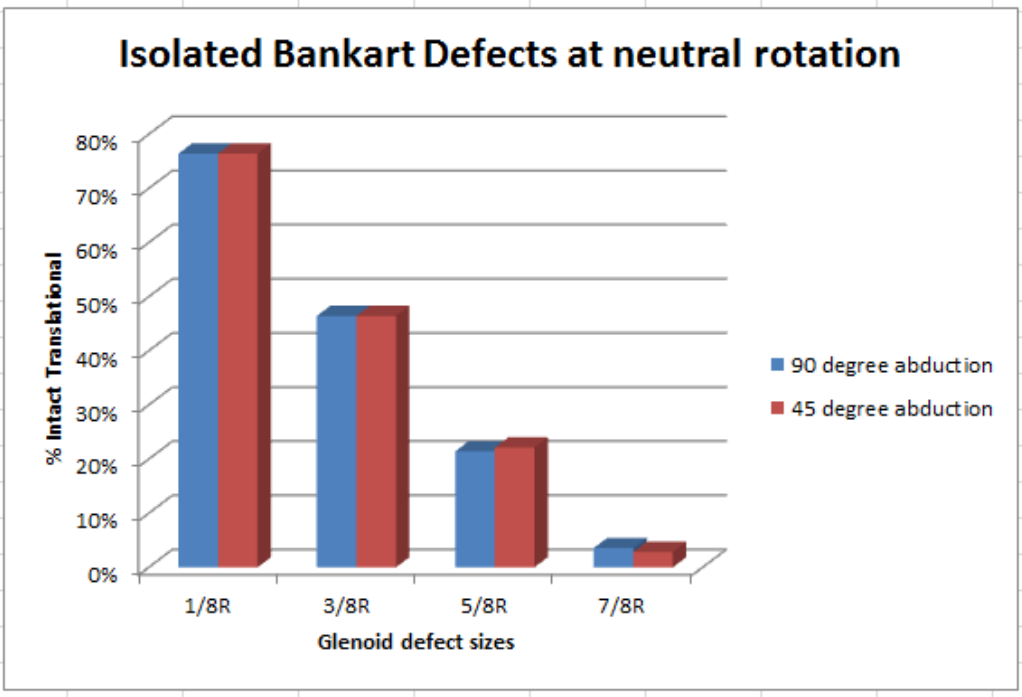

Figure 24. % Intact translation for isolated Bony Bankart lesion at both the abduction angle and neutral rotation of arm, the values are calculated with respect to the translation of intact joint.

The values for peak reaction force for both the studies were fairly similar. It can be inferred from the Figure that the value of the reaction force decreases proportional to the increase in the size of defect. It is lowest for the largest defect in both the studies.

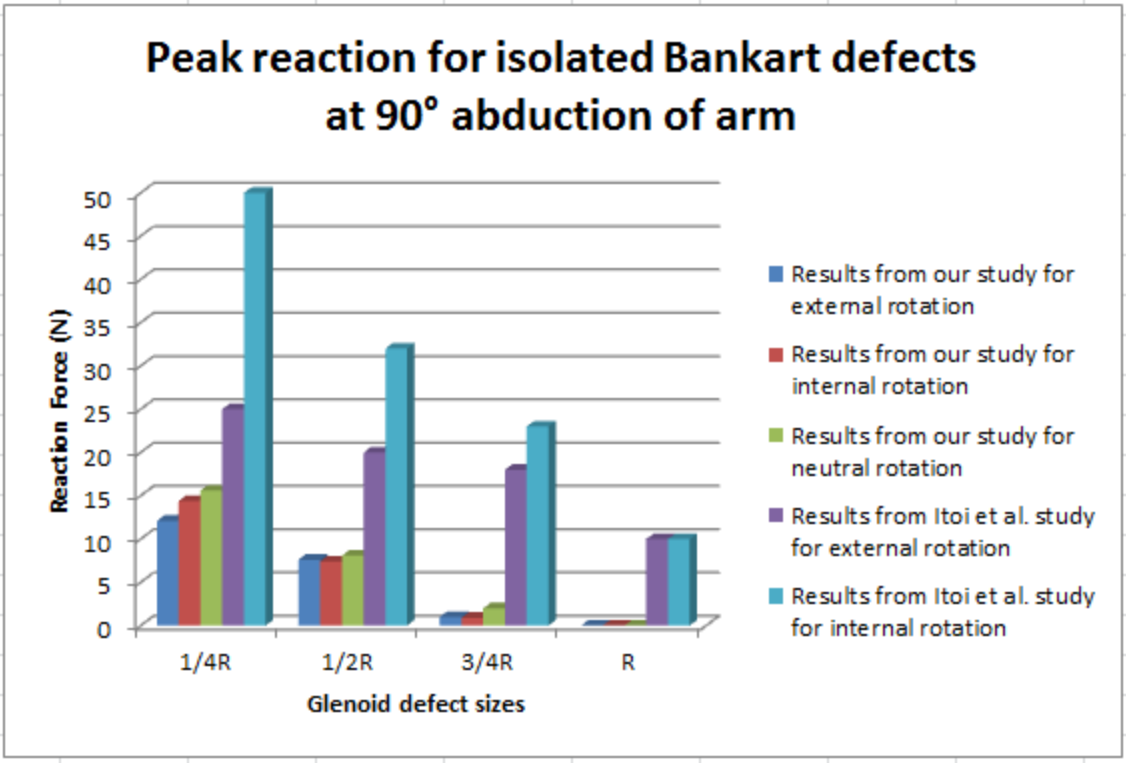

Figure 25. Net peak reaction force for the isolated Bony Bankart lesion compared with the study by Itoi et al. for 90º abduction.[27]

3.4 Results for combined defects

Figure 26 shows a 3-D plot for the distance to dislocation for the isolated and the combined Hill Sachs and Bony Bankart defects together at 90º abduction angle and neutral rotation of the arm. It can be seen that the distance to dislocation in this Figure is zero for two extreme cases, as mentioned earlier at section 2.13. Figure 27 shows the stability for all cases and combination of both lesions at 90º abduction angle. The stability ratio is zero for the largest glenoid defect and any combination with the largest glenoid defect and also it is zero for the extreme case with largest humerus defect, combined with the 3rd glenoid defect (3/4*R). Reduction in distance to dislocation is seen with the cases

of the combined defects. The stability ratio for the intact joint is 43%, which lowers down with increase in each glenoid defect and combination of the both defects. It can be seen from both Figures 26 and 27 that, distance to dislocation and stability decrease more for the increase in the size of the glenoid defect size.

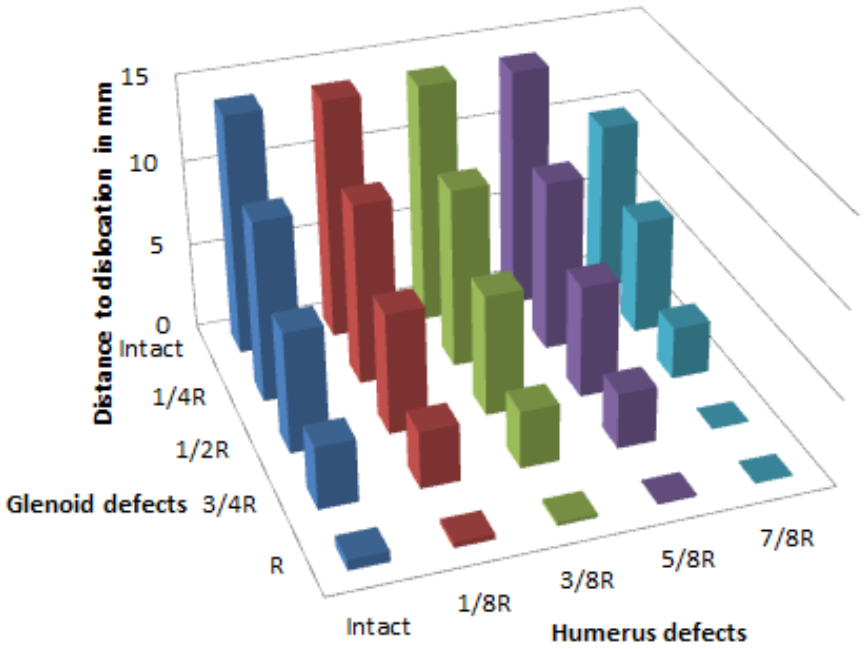

		Humerus deffects				
		Intact	**1/8R**	**3/8R**	**5/8R**	**7/8R**
Glenoid Defects	**Intact**	14	14	14	14	9.9
	1/4R	10.5	10.5	10.4	9.9	6.68
	1/2R	7	7	7	6.5	3.04
	3/4R	3.6	3.3	3.3	3.2	0
	R	0.6	0.3	0.2	0.1	0

Figure 26. Distance to dislocation for different cases at 90º abduction of arm and neutral rotation.

It can be seen clearly from the Figure 26 and 27 that the combined defects do have a significant effect on the glenohumeral joint's distance to dislocation and stability.

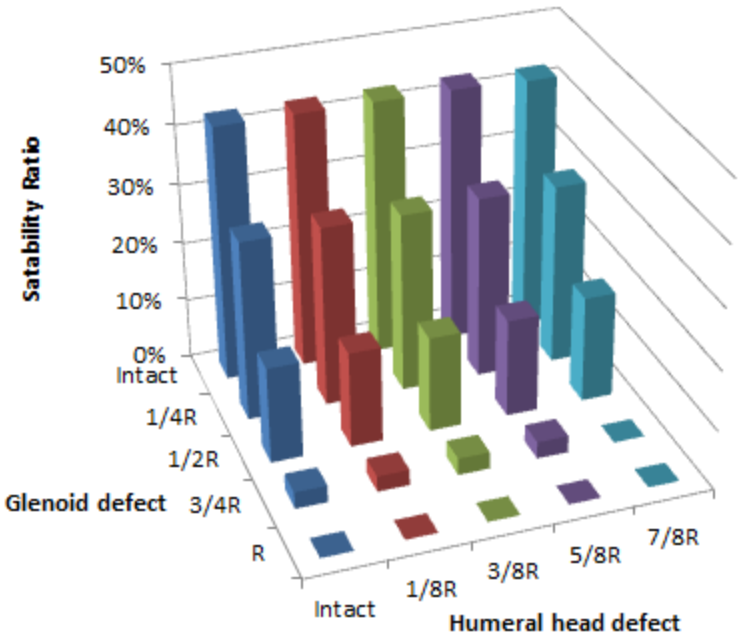

		Humerus deffects				
		Intact	**1/8R**	**3/8R**	**5/8R**	**7/8R**
Glenoid Defects	**Intact**	0.43	0.43	0.43	0.43	0.426
	1/4R	0.302	0.3026	0.301	0.306	0.304
	1/2R	0.16058	0.16	0.16	0.164	0.178
	3/4R	0.028	0.026	0.028	0.028	0
	R	0	0	0	0	0

Figure 27. Stability ratio for different cases at 90º abduction and neutral rotation of arm

The Figure 28 and 29 shows the 3-D plot for distance to dislocation and stability ratio for various cases at an arm abduction of 45º. The results show that unlike 90º abduction cases, there is no combination which has zero translational distance. The stability ratio is found to be 1% higher. The stability for the intact joint is 43% and it lowers down to nearly 0%.

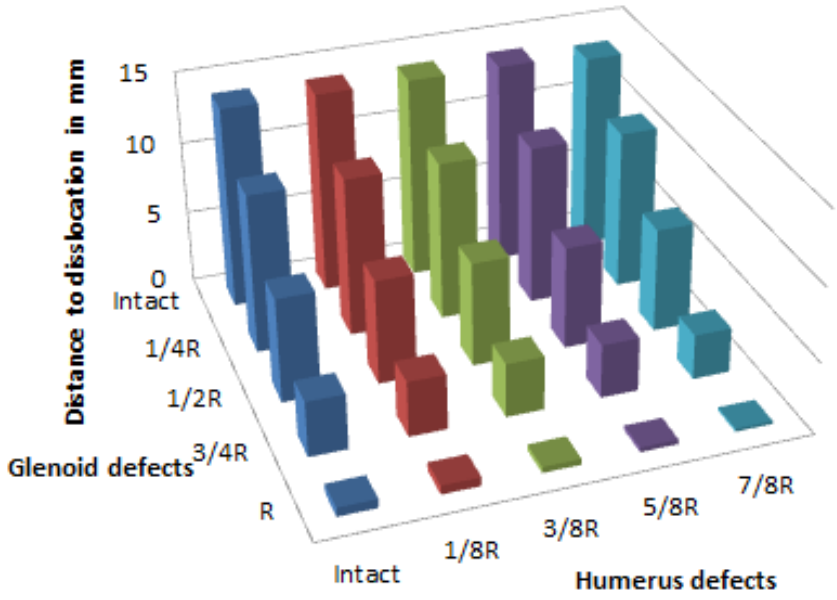

		Humerus deffects				
		Intact	1/8R	3/8R	5/8R	7/8R
Glenoid Defects	Intact	14	14	14	14	13.6
	1/4R	11	11	11	11	11
	1/2R	7.2	7.2	7.2	7.1	7.2
	3/4R	3.8	3.8	3.7	3.7	3.1
	R	0.6	0.6	0.4	0.3	0.2

Figure 28. Distance to dislocation for various cases at 45º abduction and neutral rotation of arm.

The distance to dislocation for 45° abduction and neutral rotation has been found to have very little variation with the isolated humeral head defects and lot of variation can be seen with the increasing size of the glenoid defect and different combination of both defects.

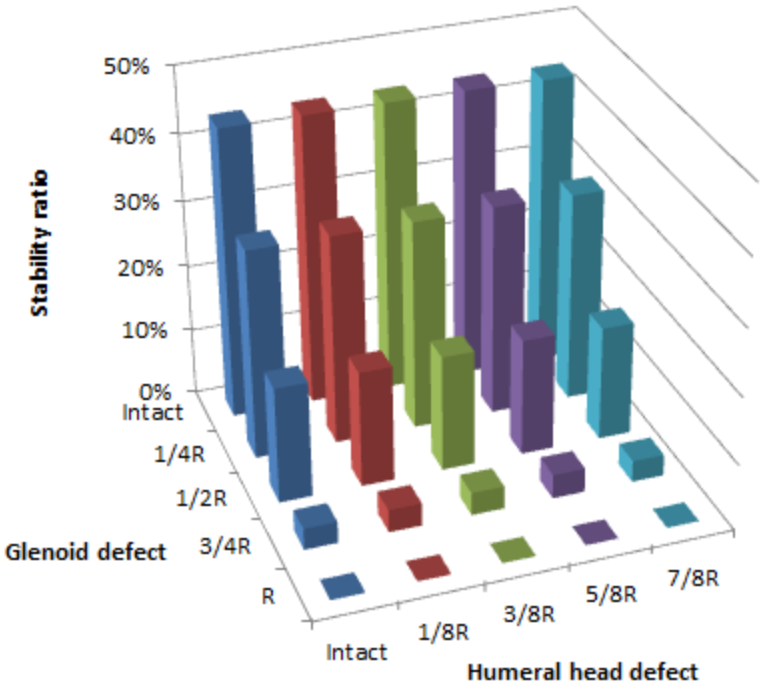

		Humerus deffects				
		Intact	1/8R	3/8R	5/8R	7/8R
Glenoid Defects	Intact	0.44	0.44	0.44	0.44	0.44
	1/4R	0.32	0.32	0.32	0.32	0.32
	1/2R	0.17	0.17	0.17	0.18	0.17
	3/4R	0.03	0.03	0.03	0.04	0.03
	R	0	0	0	0	0

Figure 29. Stability ratio for various cases at 45º abduction and neutral rotation of arm.

Figure 29 shows that the stability for the largest defect of the humerus combined with defect 1 (1/4*R) and 2 of glenoid (1/2*R) has been found to lower than that of the isolated largest defect of the glenoid.

CHAPTER IV

DISCUSSION

The purpose of this study was to evaluate the theoretical stability of the glenohumeral joint in presence of the two lesions (Bony Bankart lesion and Hill Sachs lesion under different conditions at abduction angles of 45º and 90º. The entire test study was conducted in neutral position of the arm. It was done using a finite element approach as explained in the chapter 2, which used static analysis with a simple translational test for the glenohumeral joint. The study observed the peak reaction force during the translational step and also the minimum distance required for the humerus to dislocate for each case. We hypothesized that as the size of the lesion increases, the glenohumeral joint's stability will decrease, the results from the study confirmed that our first hypothesis in almost all the cases. We further hypothesized that the presence of both defects together will reduce the glenohumeral joint's stability to an even greater extent than the presence of an individual defect. The results as shown in 3-D plots, confirmed our second hypotheses, as some of the combination of the defects reduced the stability to

approximately zero percent and also the distance to dislocation. The magnified effects were seen for translational distance to dislocation for combined defects. These results helped in understanding how the different combination of defects changes the stability and with little rotation of the arm, it may dislocate due to reduced distance to dislocation of the glenohumeral joint.

The validation of the model was one of the most important steps in the study. In order to validate our model, we compared the results from our study for the isolated defects with past studies by Itoi et al. and Kaar et al.[27, 32] As discussed in chapter 3, the Figure 21 and 22 compares the results for the % intact translation for the isolated Hill Sachs defect at 90° and 45° abduction angle and neutral rotation of the arm. The results showed the conformity with the previous study as the same pattern and values were seen with the increase in size of the defect at both the abduction angle. But the value for the largest humeral head defect at 45° abduction had a variation of 7-8% in the value the reason for which can be the approximate geometry of the glenoid and being the largest defect, the bone loos can be different as compared to other defects. The other part of the validation was to compare the results of our study for values of the peak reaction force with results from the Itoi et al. study as shown in Figure 25. We compared the results for the test conducted at 90° abduction of the arm with external and internal rotation, the only difference was that we also described the reaction force at neutral rotation of arm which shows that arm is more stable in the neutral condition than internal and external rotation. The same pattern in decrease of forces was found in both the studies and values for the reaction force for internal rotation of arm were greater than external rotation in both the studies. There was difference in the values of the reaction force which can be due to the

approximate geometry of our model and absence of the soft tissues and glenohumeral capsule, which plays a very important role in contributing to the stability of the shoulder. The similarity of the result's pattern of our study with both studies validates our model.

The results showed that the stability ratio for a normal intact glenohumeral joint is approximately 43% and 44% for 90º and 45º abduction angle respectively, but which decreased with the presence of the defect. For isolated defects in the glenoid, the stability decreased nearly to 0% for the largest defect (R) at 90º abduction and also for 45º abduction it decreased to 0%. The isolated defects in humerus did not affect the glenohumeral joint's stability for both 90º and 45º abduction of arm. The distance to dislocation is affected with both the humerus and glenoid defects, the presence of combined defects also further reduced the stability and distance to dislocation. These results have been found similar to previous studies by Kaar et al. and Itoi et al., which were used to validate our model.[27, 32] It can be inferred from the results that glenoid defects contribute more to the anterior instability of the joint. Also the distance to dislocation is majorly affected with the glenoid defect size. The presence of combined defects, i.e. the Bony Bankart and the Hill Sachs lesion, furthermore worsen the glenohumeral joint's stability. When we look at the results of the stability ratio for the joint, the Bony Bankart lesion was found to be a major cause for the glenohumeral joint's instability during abduction. The results also show that the glenohumeral joint is little more stable at 45° abduction of the arm than 90° abduction, as the stability falls to zero for combined defect with the largest humeral head defect and the third defect of the glenoid (3/4*R) at 90° abduction angle but not at 45° abduction. This was shown in 3-D plots (Figure 27) for two combination of the defect which we called the extreme cases

earlier. It is clearly seen from both the 3-D plots for distance to dislocation, that instability effects are pronounced with the combined defects of the Hill Sachs and the Bony Bankart lesion, the distance to dislocation further decreased with combination of the two defects simultaneously. No study has shown the effects of the combined defects on the stability and distance to dislocation of the joint, also stated in the study by Kaar et al.[32]

These findings represent the results for the static model of the glenohumeral joint; the future findings using this same model which will include different positions of the arm will have clinical relevance. This study provides clear and detailed information about the stability of the joint and the translational distance to dislocation for the combined defects. Itoi et al. stated in their study that defects with 21% bone loss or higher will need better repair treatments which can maintain effective length of the anterior arc of the bone. This can be done through bone grafting or by elongation of the capsoligamentous structures. But the defects below 21% percentage of bone loss can be fixed by soft tissue repairs. Similar to the results by Itoi study, Kaar et al. stated that the defect size greater than 5/8*R of the humeral head will need a surgical treatment to fix the defect; otherwise it will face the problems of recurrent instability. The results of our study showed that, with the presence of combined defects the stability further reduced to a higher degree in some of the cases. It was seen that the combination of two smaller defects had the stability lower than that of the isolated defect size stated by both the authors. Hence, the treatment options suggested by them may not be valid for some of the cases with combined defects.

The limitation of the study was the use of approximate geometry of the joint; whereas the geometry obtained from computer topography scan will reduce the errors due to approximation. The study examined glenohumeral joint instability only considering the effects due to the humerus and the glenoid, but adding the labrum into the model will predict the results better. Another limiting factor was that the experiments were done at neutral rotation with abduction of arm; but considering the external and internal rotation of the arm will give us clear understanding of the glenohumeral joint's instability while performing daily activities in our life. This consideration may furthermore prove our second hypothesis right as the humerus lesion gets in more contact with the glenoid surface, which decreases the surface area of contact for the humeral head. If we take these factors into account, the results will predict clearly about the various restriction of the arm moment depending upon the defect characteristics.

These findings give theoretical insight to the biomechanical behavior of shoulder stability in the presence of both humeral head and glenoid bone defects. This study has the potential to help surgeons to better understand the instability of this joint under different conditions of the defects if we look at the external and internal rotation of the arm. Better knowledge about these lesions will be helpful in the successful treatment options through further research, which will reduce relapse for the patient. Future directions for the study will try to look more deeply into the other factors described above. A labrum and rotator cuff will be added to the existing model and contact pressure and the stress in the system will be examined. The flexibility of FEA for our study will be an advantage, so that we can look at wider range of variables of interest and add more components easily.

REFERENCES

1. Functional Anatomy of the Shoulder, Chapter-4, p113-144. Available at: https://catalog.ama-assn.org/MEDIA/ProductCatalog/m890158/Function%20%20Anatomy%20Ch%204.pdf.

2. Allen GM. Shoulder ultrasound imaging-integrating anatomy, biomechanics and disease processes. *European Journal of Radiology.* 2008;68(1):137-146.

3. Andary JL, Petersen SA. The Vascular Anatomy of the Glenohumeral Capsule and Ligaments: An Anatomic Study. *Journal of Bone & Joint Surgery, American Volume.* 2002;84(12):2258.

4. Anderson AE, Ellis BJ, Maas SA, Peters CL, Weiss JA. Validation of finite element predictions of cartilage contact pressure in the human hip joint. *J Biomech Eng.* Oct 2008;130(5):051008.

5. Armitage MS, Faber KJ, Drosdowech DS, Litchfield RB, Athwal GS. Humeral head bone defects: Remplissage, allograft, and arthroplasty. *Orthopedic Clinics of North America.*41(3):417-425.

6. Bassett RW, Browne AO, Morrey BF, An KN. Glenohumeral muscle force and moment mechanics in a position of shoulder instability. *J Biomech.* 1990;23(5):405-415.

7. Bicos J, Mazzocca A, Romeo AA. The glenoid center line. *Orthopedics.* Jun 2005;28(6):581-585.

8. Bigliani LU, Newton PM, Steinmann SP, Connor PM, McLlveen SJ. Glenoid rim lesions associated with recurrent anterior dislocation of the shoulder. *Am J Sports Med.* Jan-Feb 1998;26(1):41-45.

9. Buchler P, Ramaniraka NA, Rakotomanana LR, Iannotti JP, Farron A. A finite element model of the shoulder: application to the comparison of normal and osteoarthritic joints. *Clin Biomech (Bristol, Avon).* Nov-Dec 2002;17(9-10):630-639.

10. Calandra JJ, Baker CL, Uribe J. The incidence of Hill-Sachs lesions in initial anterior shoulder dislocations. *Arthroscopy.* 1989;5(4):254-257.

11. Chaipat L, Palmer WE. Shoulder magnetic resonance imaging. *Clin Sports Med.* Jul 2006;25(3):371-386, v.

12. Churchill RS, Brems JJ, Kotschi H. Glenoid size, inclination, and version: an anatomic study. *J Shoulder Elbow Surg.* Jul-Aug 2001;10(4):327-332.

13. Clark J, Sidles JA, Matsen FA. The relationship of the glenohumeral joint capsule to the rotator cuff. *Clin Orthop Relat Res.* May 1990(254):29-34.

14. De Wilde LF, Berghs BM, Audenaert E, Sys G, Van Maele GO, Barbaix E. About the variability of the shape of the glenoid cavity. *Surg Radiol Anat.* Feb 2004;26(1):54-59.

15. Debski RE, Weiss JA, Newman WJ, Moore SM, McMahon PJ. Stress and strain in the anterior band of the inferior glenohumeral ligament during a simulated clinical examination. *J Shoulder Elbow Surg.* Jan-Feb 2005;14(1 Suppl S):24S-31S.

16. Di Giacomo G. *Atlas of functional shoulder anatomy [electronic resource] / Giovanni Di Giacomo ... [et al.], editors*. Milan ; New York :: Springer; 2008.

17. Edwards TB, Boulahia A, Walch G. Radiographic analysis of bone defects in chronic anterior shoulder instability. *Arthroscopy.* Sep 2003;19(7):732-739.

18. Ellis BJ, Debski RE, Moore SM, McMahon PJ, Weiss JA. Methodology and sensitivity studies for finite element modeling of the inferior glenohumeral ligament complex. *J Biomech.* 2007;40(3):603-612.

19. Flinkkila T, Hyvonen P, Ohtonen P, Leppilahti J. Arthroscopic Bankart repair: results and risk factors of recurrence of instability. *Knee Surg Sports Traumatol Arthrosc.* Mar 27 2010.

20. Fox JA, Cole BJ, Romeo AA, et al. Articular cartilage thickness of the humeral head: an anatomic study. *Orthopedics.* Mar 2008;31(3):216.

21. Freeman MAR, ed. *Adult Articular Cartilage.* 2nd ed: Pitman medical; 1979. Kempson GE, ed. Mechanical properties of articular cartilage, p-333-414.

22. Hill HA, Sachs MD. The Grooved Defect of the Humeral Head. *Radiology.* December 1, 1940 1940;35(6):690-700.

23. Hopkins AR, Hansen UN, Amis AA, Taylor M, Gronau N, Anglin C. Finite element modelling of glenohumeral kinematics following total shoulder arthroplasty. *J Biomech.* 2006;39(13):2476-2483.

24. Howell SM, Galinat BJ, Renzi AJ, Marone PJ. Normal and abnormal mechanics of the glenohumeral joint in the horizontal plane. *J Bone Joint Surg Am.* Feb 1988;70(2):227-232.

25. Hubsch PF, Middleton J, Meroi EA, Natali AN. Adaptive finite-element approach for analysis of bone/prosthesis interaction. *Med Biol Eng Comput.* Jan 1995;33(1):33-37.

26. Iannotti JP, Gabriel JP, Schneck SL, Evans BG, Misra S. The normal glenohumeral relationships. An anatomical study of one hundred and forty shoulders. *J Bone Joint Surg Am.* Apr 1992;74(4):491-500.

27. Itoi E, Lee SB, Berglund LJ, Berge LL, An KN. The effect of a glenoid defect on anteroinferior stability of the shoulder after Bankart repair: a cadaveric study. *J Bone Joint Surg Am.* Jan 2000;82(1):35-46.

28. Izquierdo R, Voloshin I, Edwards S, et al. Treatment of glenohumeral osteoarthritis. *J Am Acad Orthop Surg.* Jun 2010;18(6):375-382.

29. Jeong J, Bryan J, Iannotti JP. Effect of a variable prosthetic neck-shaft angle and the surgical technique on replication of normal humeral anatomy. *J Bone Joint Surg Am.* Aug 2009;91(8):1932-1941.

30. Jeske H-C, Oberthaler M, Klingensmith M, et al. Normal glenoid rim anatomy and the reliability of shoulder instability measurements based on intrasite correlation. *Surgical & Radiologic Anatomy.* 2009;31(8):623-625.

31. Jobe CM, Iannotti JP. Limits imposed on glenohumeral motion by joint geometry. *J Shoulder Elbow Surg.* Jul-Aug 1995;4(4):281-285.

32. Kaar SG, Fening SD, Jones MH, Colbrunn RW, Miniaci A. Effect of humeral head defect size on glenohumeral stability: a cadaveric study of simulated Hill-Sachs defects. *Am J Sports Med.* Mar;38(3):594-599.

33. Kelkar R, Wang VM, Flatow EL, et al. Glenohumeral mechanics: a study of articular geometry, contact, and kinematics. *J Shoulder Elbow Surg.* Jan-Feb 2001;10(1):73-84.

34. Kronberg M, Brostrom LA, Soderlund V. Retroversion of the humeral head in the normal shoulder and its relationship to the normal range of motion. *Clin Orthop Relat Res.* Apr 1990(253):113-117.

35. Kuechle DK, Newman SR, Itoi E, Morrey BF, An KN. Shoulder muscle moment arms during horizontal flexion and elevation. *J Shoulder Elbow Surg.* Sep-Oct 1997;6(5):429-439.

36. Kwon YW, Powell KA, Yum JK, Brems JJ, Iannotti JP. Use of three-dimensional computed tomography for the analysis of the glenoid anatomy. *J Shoulder Elbow Surg.* Jan-Feb 2005;14(1):85-90.

37. Levine WN, Flatow EL. The Pathophysiology of Shoulder Instability. *American Journal of Sports Medicine.* 2000;28(6):910.

38. Lippitt S, Matsen F. Mechanisms of glenohumeral joint stability. *Clin Orthop Relat Res.* Jun 1993(291):20-28.

39. Mallon WJ, Brown HR, Vogler JB, 3rd, Martinez S. Radiographic and geometric anatomy of the scapula. *Clin Orthop Relat Res.* Apr 1992(277):142-154.

40. Mansat P, Barea C, Hobatho MC, Darmana R, Mansat M. Anatomic variation of the mechanical properties of the glenoid. *J Shoulder Elbow Surg.* Mar-Apr 1998;7(2):109-115.

41. McCluskey GM, Getz BA. Pathophysiology of anterior shoulder instability. *J Athl Train.* Jul 2000;35(3):268-272.

42. Meller R, Krettek C, GÃ¶sling T, WÃ¤hling K, Jagodzinski M, Zeichen J. Recurrent shoulder instability among athletes: Changes in quality of life, sports activity, and muscle function following open repair. *Knee Surgery, Sports Traumatology, Arthroscopy.* 2007;15(3):295-304.

43. Merila M, Leibecke T, Gehl HB, et al. The anterior glenohumeral joint capsule: macroscopic and MRI anatomy of the fasciculus obliquus or so-called ligamentum glenohumerale spirale. *European Radiology.* 2004;14(8):1421-1426.

44. Merrill A, Guzman K, Miller SL. Gender differences in glenoid anatomy: an anatomic study. *Surgical & Radiologic Anatomy.* 2009;31(3):183-189.

45. Moore SM, Ellis B, Weiss JA, McMahon PJ, Debski RE. The glenohumeral capsule should be evaluated as a sheet of fibrous tissue: a validated finite element model. *Ann Biomed Eng.* Jan;38(1):66-76.

46. O'Brien SJ, Neves MC, Arnoczky SP, et al. The anatomy and histology of the inferior glenohumeral ligament complex of the shoulder. *The American Journal of Sports Medicine.* September 1990 1990;18(5):449-456.

47. Ogawa K, Yoshida A, Matsumoto H, Takeda T. Outcome of the open Bankart procedure for shoulder instability and development of osteoarthritis: A 5- to 20-year follow-up study. *American Journal of Sports Medicine.*38(8):1549-1557.

48. Owens BD, Dawson L, Burks R, Cameron KL. Incidence of shoulder dislocation in the United States military: Demographic considerations from a high-risk population. *Journal of Bone and Joint Surgery - Series A.* 2009;91(4):791-796.

49. Pearl ML, Volk AG. Coronal plane geometry of the proximal humerus relevant to prosthetic arthroplasty. *J Shoulder Elbow Surg.* Jul-Aug 1996;5(4):320-326.

50. Prendergast PJ. Finite element models in tissue mechanics and orthopaedic implant design. *Clin Biomech (Bristol, Avon).* Sep 1997;12(6):343-366.

51. Richmond BG, Wright BW, Grosse I, et al. Finite element analysis in functional morphology. *Anat Rec A Discov Mol Cell Evol Biol.* Apr 2005;283(2):259-274.

52. Rowe CR, Patel D, Southmayd WW. The Bankart procedure: a long-term end-result study. *J Bone Joint Surg Am.* Jan 1978;60(1):1-16.

53. Rowe CR, Zarins B, Ciullo JV. Recurrent anterior dislocation of the shoulder after surgical repair. Apparent causes of failure and treatment. *J Bone Joint Surg Am.* Feb 1984;66(2):159-168.

54. Sam W. Wiesel JND. *Essentials of orthopedic surgery / edited by Sam W. Wiesel, John N. Delahay*. 3rd ed ed. New York :: Springer; 2007.

55. Schonning A, Oommen B, Ionescu I, Conway T. Hexahedral mesh development of free-formed geometry: The human femur exemplified. *Computer-Aided Design.* 2009;41(8):566-572.

56. Sekiya JK, Wickwire AC, Stehle JH, Debski RE. Hill-Sachs defects and repair using osteoarticular allograft transplantation: biomechanical analysis using a joint compression model. *Am J Sports Med.* Dec 2009;37(12):2459-2466.

57. Sizer PS, Phelps V, Gilbert K. Diagnosis and Management of the Painful Shoulder. Part 1: Clinical Anatomy and Pathomechanics. *Pain Practice.* 2003;3(1):39-57.

58. Soslowsky LJ, Flatow EL, Bigliani LU, Mow VC. Articular geometry of the glenohumeral joint. *Clin Orthop Relat Res.* Dec 1992(285):181-190.

59. Terry GC, Chopp TM. Functional Anatomy of the Shoulder. *Journal of Athletic Training.* 2000;35(3):248.

60. Turkel SJ, Panio MW, Marshall JL, Girgis FG. Stabilizing mechanisms preventing anterior dislocation of the glenohumeral joint. *J Bone Joint Surg Am.* Oct 1981;63(8):1208-1217.

61. von Eisenhart-Rothe R, Mayr HO, Hinterwimmer S, Graichen H. Simultaneous 3D assessment of glenohumeral shape, humeral head centering, and scapular positioning in atraumatic shoulder instability: a magnetic resonance-based in vivo analysis. *Am J Sports Med.* Feb;38(2):375-382.

62. Wang RY, Arciero RA. Treating the athlete with anterior shoulder instability. *Clin Sports Med.* Oct 2008;27(4):631-648.

63. Wataru S, Kazuomi S, Yoshikazu N, Hiroaki I, Takaharu Y, Hideki Y. Three-dimensional morphological analysis of humeral heads: a study in cadavers. *Acta Orthop.* Jun 2005;76(3):392-396.

64. Widjaja AB, Tran A, Bailey M, Proper S. Correlation between bankart and Hill-Sachs lesions in anterior shoulder dislocation. *ANZ Journal of Surgery.* 2006;76(6):436-438.

65. Wilson SR. Dislocation, Shoulder: EMedicine Emergency Medicine. *EMedicine - Medical Reference.* 14 Dec. 2009:Web. 01 Nov. 2010.

66. Xu W, Crocombe AD, Hughes SC. Finite element analysis of bone stress and strain around a distal osseointegrated implant for prosthetic limb attachment. *Proc Inst Mech Eng H.* 2000;214(6):595-602.

67. Yamamoto N, Itoi E, Abe H, et al. Effect of an anterior glenoid defect on anterior shoulder stability: a cadaveric study. *Am J Sports Med.* May 2009;37(5):949-954.

68. Yeh LR, Kwak S, Kim YS, et al. Evaluation of articular cartilage thickness of the humeral head and the glenoid fossa by MR arthrography: anatomic correlation in cadavers. *Skeletal Radiol.* Sep 1998;27(9):500-504.

69. Zhang L, Wang J, Wang C. [Function study for finite element analysis of AB-IGHL during humeral external rotation]. *Sheng Wu Yi Xue Gong Cheng Xue Za Zhi.* Jun 2009;26(3):504-507.